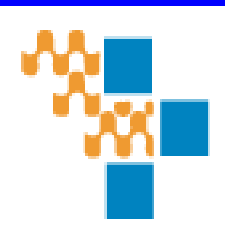




Validació de biomarcadors d'imatge en medicina



5a Jornada
de Recerca a
l'Institut Català
de la Salut

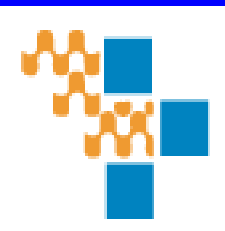




Salvador Pedraza

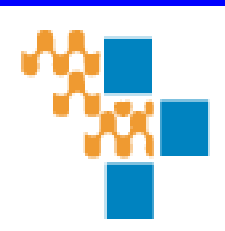
Grup recerca Imatge Mèdica. IDIBGI.

**Centre IDI-Servei de Radiologia
Hospital Dr. Josep Trueta**





Validació de Biomarcadors Imatge



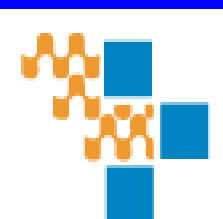


INTERNATIONAL DAY OF RADIOLOGY

AN INITIATIVE OF THE ESR, ACR AND RSNA

Let's celebrate together
November 8, 2012

						
						
About IDoR	Participating Societies	Activities	Publications	Videos	Press & PR	



Radiologia

Gran èxit de la Radiologia.

**“L'avanç més important de la Medicina
en els últims 100 anys”**

(TC-RM)”. (JAMA).

Futur Medicina

- **Diagnòstic precoç.**
- **Personalització en cada malaltia del tractament.**
- **Desenvolupament de biomarcadors d'imatge.**
- **Imatge Molecular.**

Opinion

John J. Smith, MD, JD
A. Gregory Sorensen, MD
James H. Thrall, MD

Index terms:

Opinions
Radiology and radiologists, research
Radiology and radiologists,
socioeconomic issues

Published online before print

10.1148/radiol.2273020518
Radiology 2003; 227:633–638

Abbreviation:

FDA = Food and Drug
Administration

¹ From the Department of Radiology and MGH Center for Biomarkers in Imaging, Massachusetts General Hospital, 15 Parkman St, WACC 515, Boston, MA 02114. Received May 6, 2002; revision requested July 10; revision received August 13; accepted October 1. **Address correspondence to J.J.S.** (e-mail: smith.john@mgh.harvard.edu).

Biomarkers in Imaging: Realizing Radiology's Future¹

Modern pharmaceuticals and medical devices have provided substantial benefits to patients throughout the world. These benefits come at a high and increasing cost, with development of the typical pharmaceutical requiring 12 years and hundreds of millions of dollars before gaining U.S. Food and Drug Administration marketing approval. Appropriate use of imaging biomarkers—defined as anatomic, physiologic, biochemical, or molecular parameters detectable with imaging methods used to establish the presence or severity of disease—offer the prospect of smaller, less expensive, and more efficient preclinical studies and clinical trials. Scientists, government regulators, and industry have all recognized the potential of biomarkers in imaging. Although real, this promise can only be realized with the rigorous application of science to their use. Success is most likely when (a) the presence of an imaging marker is closely linked with the presence of a target disease; (b) detection and/or measurement of the biomarker is accurate, reproducible, and feasible over time; and (c) measured changes are closely linked to success or failure of the therapeutic effect of the product being evaluated. By applying this paradigm to the array of imaging modalities, the radiology community is poised to become a major force in preclinical and clinical evaluations of new medical treatments.

© RSNA, 2003

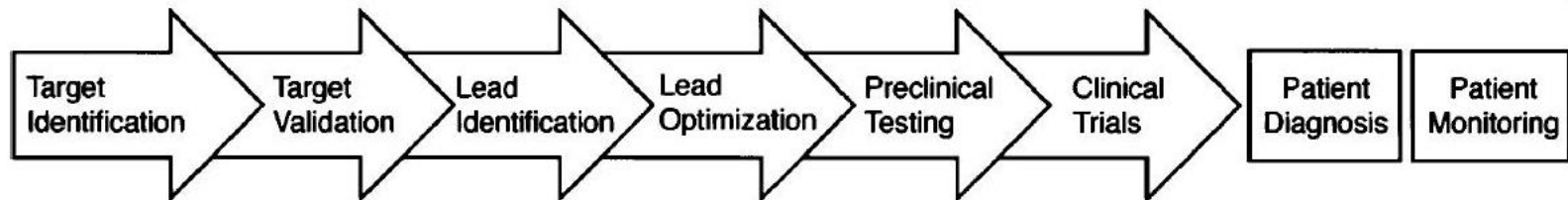
Definició

- **“Anatomic, physiologic, biochemical, or molecular parameters**
- **detectable with imaging methods**
- **used to establish the presence or severity of disease**
- **offer the prospect of smaller, less expensive, and more efficient preclinical studies and clinical trials”.**

Gran Potencial

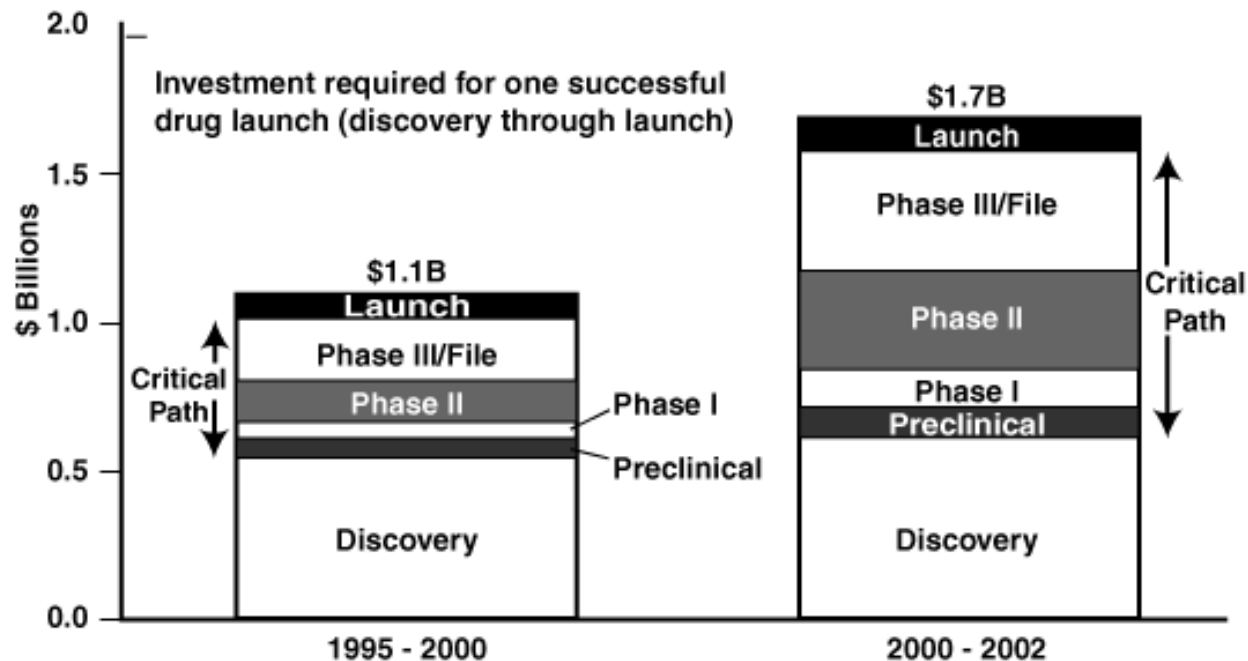
- Success is most likely when:
- *(a) the presence of an imaging marker is closely linked with the presence of a target disease;*
- *(b) detection and/or measurement of the biomarker is accurate, reproducible, and feasible over time;*
- *(c) measured changes are closely linked to success or failure of the therapeutic effect of the product being evaluated.*

Procés de Validació de BI



Typical industrial product-development pathway outlines steps necessary to initially identify a promising site of therapeutic action and potential therapy that affects that site and then validate that therapy for clinical use. In this diagram, targets are typically molecular steps or events in the physiology or pathophysiology that could be targeted with new therapies, such as a receptor or a signal transduction pathway. "Leads" are novel compounds or devices that might act on such targets.

Augment del cost d'aprovació de nous tractaments



Biomarcador d'Imatge



- Is the effort to stimulate and facilitate a national effort to modernize the scientific process through which a potential human drug, biological product, or medical device is transformed from a.. discovery or "proof of concept" into a medical product

Biomarcador d'Imatge

TABLE 1
Roles of Imaging Biomarkers

Product Development Stage	Applicability of Imaging Biomarkers	Imaging Modality
Target identification	Yes	Nuclear medicine, PET, other molecular imaging approaches
Target validation	Yes	Nuclear medicine, PET, other molecular imaging approaches
Lead identification	No	None
Lead optimization	Yes	Nuclear medicine, PET, other molecular imaging approaches
Preclinical testing	Yes	Nuclear medicine, PET, other molecular imaging, CT, MR
Clinical trials	Yes	CT, MR, US, nuclear medicine, PET, conventional radiography
Diagnosis	Yes	CT, MR, US, nuclear medicine, PET, conventional radiography
Patient monitoring	Yes	CT, MR, US, nuclear medicine, PET, conventional radiography

Note.—PET = positron emission tomography, US = ultrasonography.

Biomarcador d'Imatge

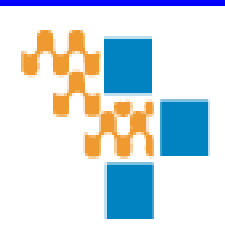
TABLE 2
Biomarkers in Imaging versus True or Traditional End Points

Parameter	True or Traditional Endpoints	Imaging Biomarkers
Time frame to results	May be long, particularly when mortality used	Potential for substantially shorter results time frame
Objectivity	May be low when morbidity or similarly subjective end point is used	Potential for increased objectivity where end points other than mortality are used
Cost	High, particularly when mortality or other long-term end point is used	Relatively low compared with long-term true or traditional end points
Ability to achieve blinding	May be difficult, particularly with medical devices	Relatively easy in the setting of blinded readers
Ability to detect subtle change	Often low	Routine ability to detect small changes on images
Ability of patient to serve as own control	Possible, but may be difficult in practice	Possible in many instances
Access to required resources	Widespread but expensive, dedicated infrastructure required	Widespread, with cost of imaging infrastructure largely defrayed by routine clinical use

Smith JJ et al. Radiology 2003; 227:633-638.



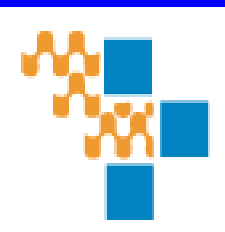
Infart cerebral
Tumor cerebral
Hidrocefalia
Síndrome metabòlic.
Malaltia discal





Validació Biomarcadors d' Imatge

Infart cerebral

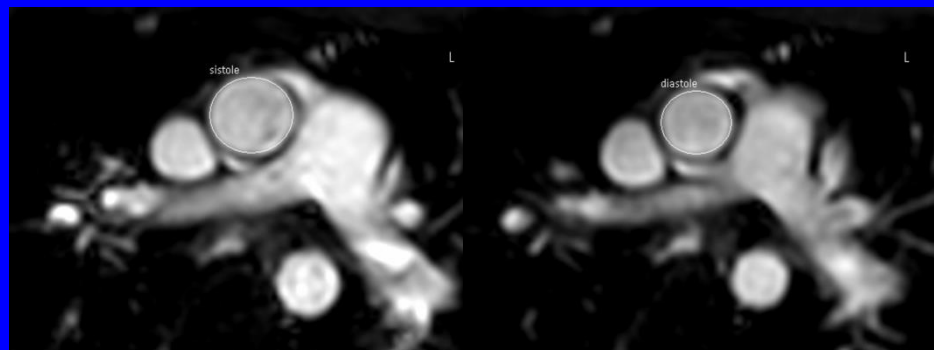




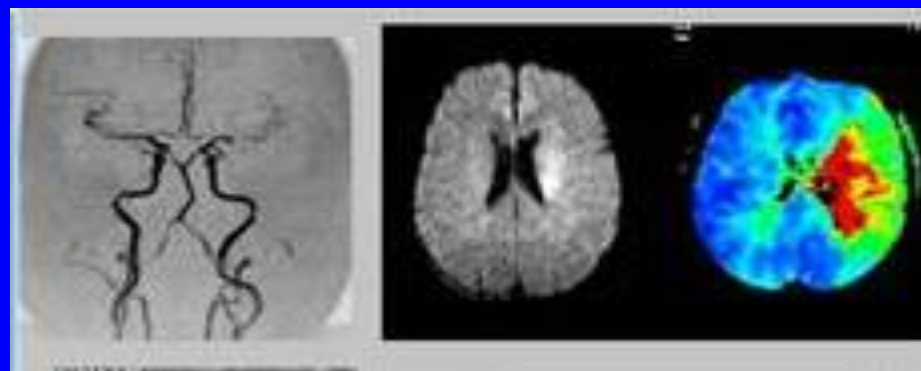
INFART CEREBRAL



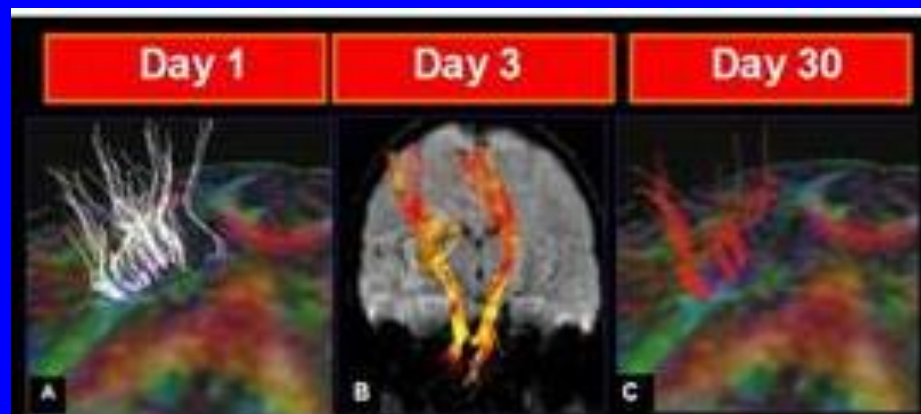
Prevenció Infart



Infart agut



Infart crònic

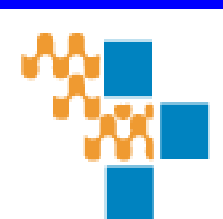
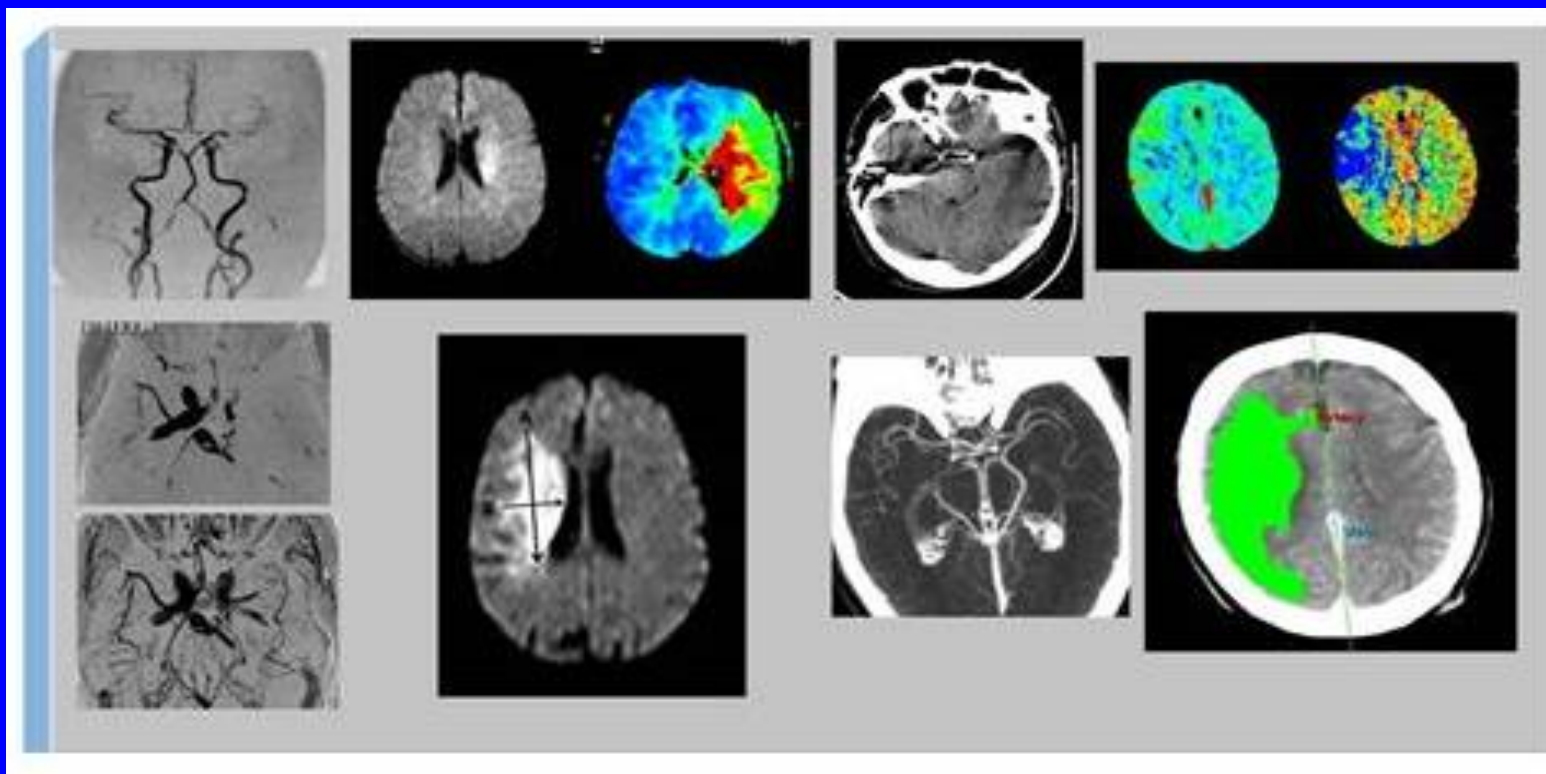




INFART CEREBRAL



Valoració per RM i TC



Expert Opinion

1. Introduction
2. Review of diagnostic imaging in stroke
3. Conclusions
4. Expert opinion

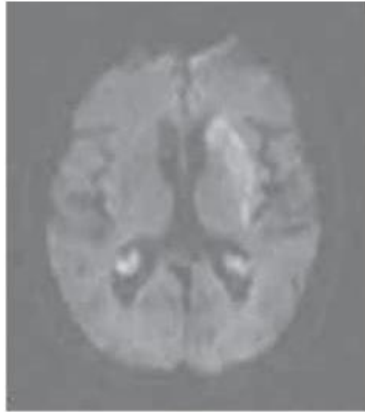
Magnetic resonance imaging in the diagnosis of stroke

Salvador Pedraza[†], Josep Puig, Sebastian Remollo, Ana Quiles, Eva Gomez, Gemma Laguillo & Gerard Blasco

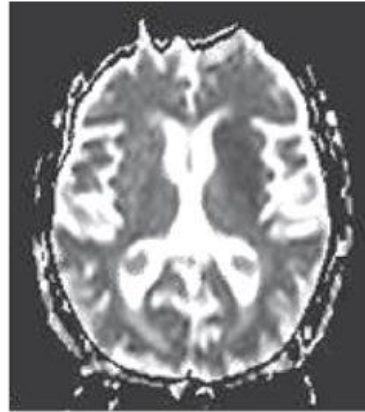
Hospital Universitario Dr Josep Trueta, Centro de RM, IDI, Servicio de Radiología, Av de Francia sn, 17007, Girona, Spain

Background: The high morbidity and mortality of strokes result in enormous costs to our society. In the last decade advanced imaging techniques with high sensitivity in the diagnosis of acute stroke have been developed. Acute thrombolytic treatment beyond 3 h of acute stroke duration requires the demonstration of penumbra or 'tissue at risk'. However, the utility of the mismatch concept to identify the penumbra area is controversial. **Objective:** The aim is to describe the main features of acute stroke on magnetic resonance imaging. **Method:** Information was obtained from a search of the PubMed and Medline databases (keywords: imaging, stroke, diagnosis and infarct) for articles published from 1997. **Conclusion:** To conclude, new imaging biomarkers of relevant mismatch, hemorrhagic transformation and worse outcome should be developed in the future.

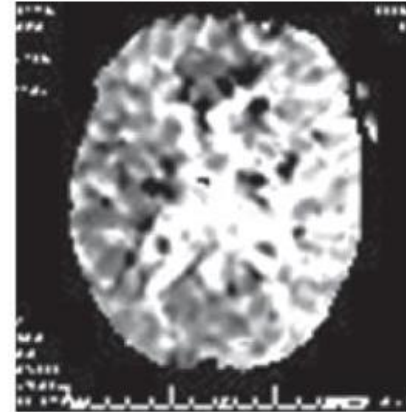
Protocol d'imatge de l'Infart.



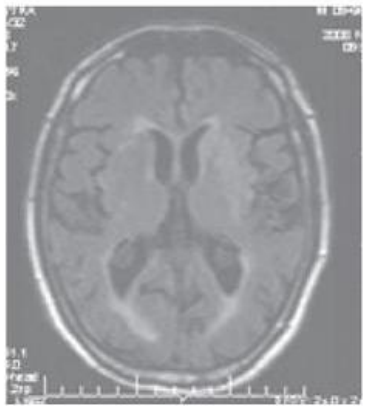
DWI



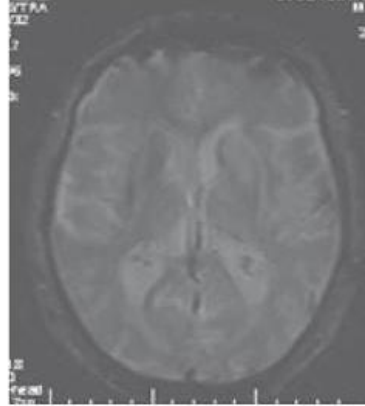
ADC



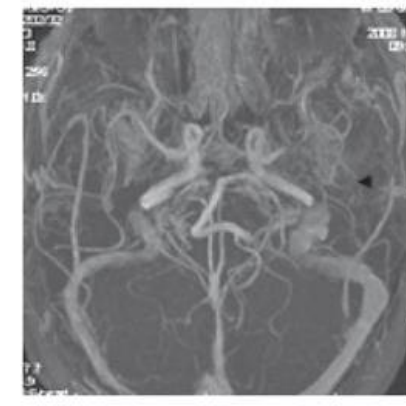
MTT



FLAIR



T2GE



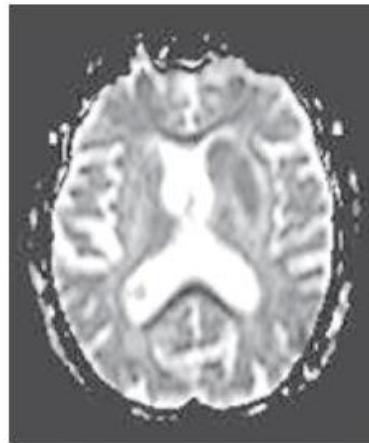
MRA

Pedraza S et al. Magnetic resonance imaging in the diagnosis of Stroke. Expert Opin. Med. Diagn. 2008; 2(7): 1-10.

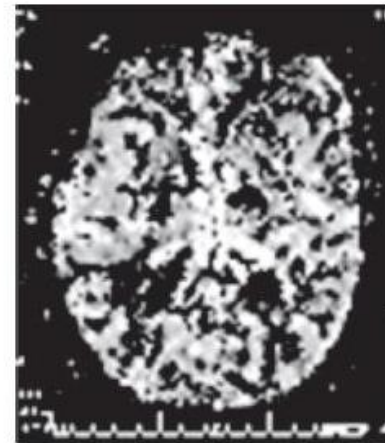
Protocol d'imatge de l'Infart.



DWI



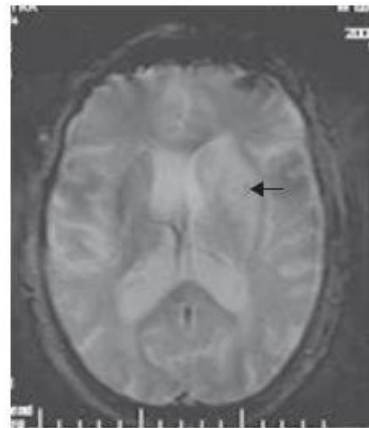
ADC



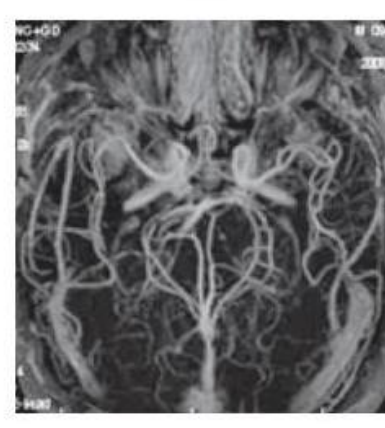
MTT



FLAIR



T2GE



MRA

Pedraza S et al. Magnetic resonance imaging in the diagnosis of Stroke. Expert Opin. Med. Diagn. 2008; 2(7): 1-10.

FOCUS ON BIOMARKERS

MAGNETIC RESONANCE IMAGING BIOMARKERS OF ISCHEMIC STROKE: CRITERIA FOR THE VALIDATION OF PRIMARY IMAGING BIOMARKERS

by Salvador Pedraza, Josep Puig, Gerard Blasco, Josep Daunis-I-Estadella, Imma Boada, Anton Bardera, Alberto Prats, Mar Castellanos and Joaquín Serena

ing (MRI) has an established role in the study of acute stroke patients (Fig. 1).¹¹ Different MRI techniques are useful in the study of acute stroke. Magnetic resonance angiography (MRA) can evaluate a patient's vascular status. Diffusion-weighted imaging (DWI) and T2*-weighted sequences can dif-

Further large, randomized trials will enable us to overcome the limitations of current MRI biomarkers of acute ischemic stroke and validate new biomarkers.

SUMMARY

Ischemic stroke is associated with a high rate of disability and death. Establishing valid biomarkers could help accelerate the approval of promising new therapies for stroke. Whereas

Definició de criteris de validesa de un biomarcador d'Imatge en l'Infart

Table 1. Set of criteria for a valid magnetic resonance imaging (MRI) biomarker of stroke

1. The biomarker should be a biological, physiological, biochemical or anatomical change detectable with MRI.
2. The biomarker should be closely linked with the target of the disease treatment.
3. The biomarker should have a logical relationship with the severity of the disease. It is important to have a strong link to the true endpoint.
4. The detection and/or quantitative measurement of the biomarker should be accurate, reproducible and feasible.
5. New treatments (drugs or devices) can change the biomarker's value. The measured changes over time are closely linked to the success or failure of the therapy and to the true endpoint of the medical therapy being evaluated.
6. The biomarker can provide insight into the toxicity of a treatment.
7. Some MRI biomarkers are supported by a large body of scientific evidence and are thus highly recommended for clinical use in acute stroke. Preclinical assessment is valuable.

Pedraza S et al. MRI Biomarkers of ischemic stroke: Criteria for the validation of primary imaging biomarkers. Drug News perspective 2009; 22 (8).

Classificació de Biomarcadors de Imatge en l'Infart.

A. Symptomatic vessel patency

Initial vessel patency, final vessel status, early recanalization, late recanalization.

B. Infarct lesion volume

Initial infarct volume, final lesion volume, lesion enlargement between days 1 and 3, lesion enlargement between days 1 and 30.

C. Reversibility of acute ischemic lesion

Diffusion-weighted imaging reversibility.

D. Perfusion alteration

Initial perfusion alteration, final perfusion alteration, early reperfusion, late reperfusion.

E. Penumbra volume determined as diffusion-perfusion mismatch

F. Penumbra volume determined as clinical-diffusion mismatch

G. Penumbra volume determined as diffusion-angiography mismatch

H. Hemorrhagic transformation of acute infarct

Grades of hemorrhagic transformation.

Pedraza S et al. MRI Biomarkers of ischemic stroke: Criteria for the validation of primary imaging biomarkers. Drug News perspective 2009; 22 (8).

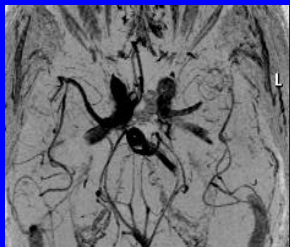
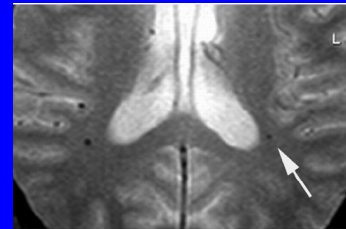
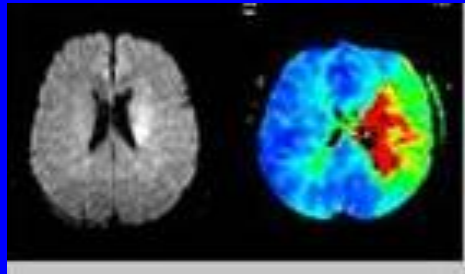
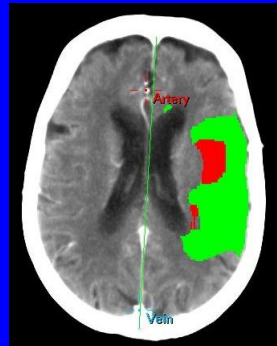
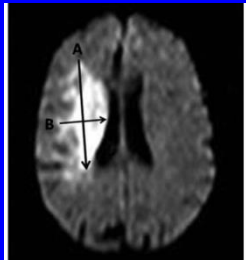
Grau de validesa de cadascun dels Biomarcadors d' Imatge en l'Infart cerebral.

Table III. Validity of each MRI-BAS

MRI change	Vessel patency +++	Infarct lesion volume +++	DWI reversal +++	Perfusion alteration +++	PWI-PWI mismatch +++	CDM +++	DWI-MRA mismatch +++	Hemorrhagic transformation +++
Target	+++			++	++	++	++	
Correlation with severity of disease	+	+	+	+	+	+	+	+
Quality quantitative measurement	+	+	+	+	+	+	+	+
Treatments change value of MRI-BAS	+++	++	++	+++	+++	+++	+++	++
Inclusion criteria	+				+++		+	
Exclusion criteria	+++	+			+++			+++
Secondary endpoint	+++	+++		+++				++
Toxicity assessment								+++
Evidence in publications	+	+	+	+	+	+	+	+

Pedraza S et al. MRI Biomarkers of ischemic stroke: Criteria for the validation of primary imaging biomarkers. Drug News perspective 2009; 22 (8).

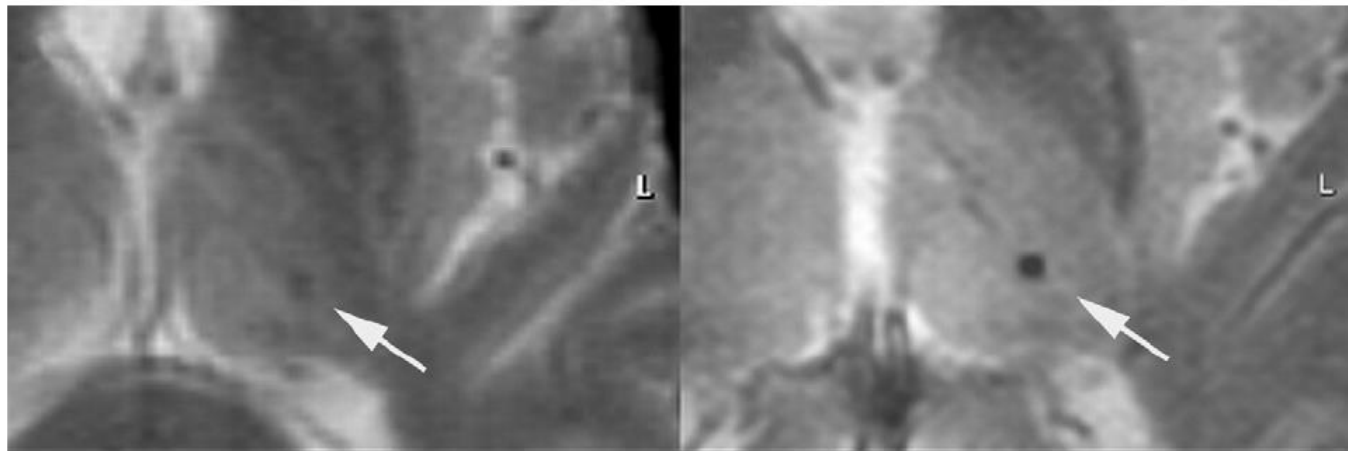
Vessel patency	Infarct lesion volume	DWI reversal	Perfusion alteration	PWI-PWI mismatch	CDM	DWI-MRA mismatch	Hemorrhagic transformation
-------------------	-----------------------------	-----------------	-------------------------	---------------------	-----	---------------------	-------------------------------



**Validació,
Qualificació**

Microhemorragias

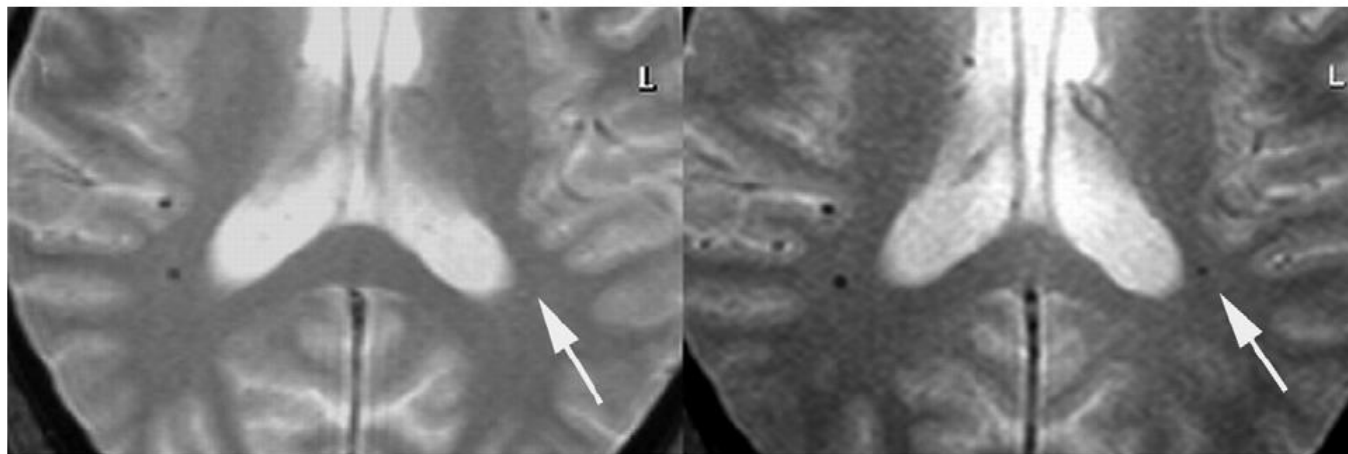
Microbleeds



a.

b.

Figure 2. Cerebral microbleed (CMB) at 1.5 (a) and 3.0 T (b). At 1.5 T, the CMB (*white arrow*) in the capsula interna is brighter and has a lower CNR compared to 3.0 T.



a.

b.

Figure 3. At 1.5 T, the cerebral microbleeds in the right periventricular white matter is brighter and has a lower CNR. The cerebral microbleed in the left periventricular white matter (*white arrow*) is not visible on 1.5 T (a) but on 3.0 T (b).

Stroke

JOURNAL OF THE AMERICAN HEART ASSOCIATION

American Stroke
AssociationSM

A Division of American
Heart Association



**Bleeding Risk Analysis in Stroke Imaging Before ThromboLysis (BRASIL).
Pooled Analysis of T2*-Weighted Magnetic Resonance Imaging Data From 570
Patients**

Jens Fiehler, Gregory W. Albers, Jean-Martin Boulanger, Laurent Derex, Achim Gass,
Niels Hjort, Jong S. Kim, David S. Liebeskind, Tobias Neumann-Haefelin, Salvador
Pedraza, Joachim Rother, Peter Rothwell, Alex Rovira, Peter D. Schellinger, Johannes
Trenkler and for the MR STROKE Group

Stroke published online Aug 23, 2007;

DOI: 10.1161/STROKEAHA.106.480848

Stroke is published by the American Heart Association, 7272 Greenville Avenue, Dallas, TX 75214
Copyright © 2007 American Heart Association. All rights reserved. Print ISSN: 0039-2499. Online
ISSN: 1524-4628

TABLE 2. Numbers of CMBs in Patients Without Clinical Deterioration and Hemorrhage (No HE), With Clinical Deterioration but Without PH (Any HE), and With SICH on Follow-Up Imaging

CMB No.	No HE	Any HE	SICH	Total
0	455	29	13	484
1	46	4	3	50
2	17	2	0	19
3	8	0	0	8
4	2	0	0	2
5	2	0	0	2
6	1	0	0	1
7	0	1	1	1
8	1	0	0	1
14	1	0	0	1
77	0	1	1	1
Total	533	37	18	570

Fiehler J et al. Stroke 2007;38: 2738-44.

Bleeding Risk Analysis in Stroke Imaging Before ThromboLysis (BRASIL)

Pooled Analysis of T2*-Weighted Magnetic Resonance Imaging Data From 570 Patients

Jens Fiehler, MD; Gregory W. Albers, MD; Jean-Martin Boulanger, MD; Laurent Derex, MD; Achim Gass, MD; Niels Hjort, MD; Jong S. Kim, MD; David S. Liebeskind, MD; Tobias Neumann-Haefelin, MD; Salvador Pedraza, MD; Joachim Rother, MD; Peter Rothwell, MD, PhD; Alex Rovira, MD; Peter D. Schellinger, MD; Johannes Trenkler, MD; for the MR STROKE Group

Background and Purpose—There has been speculation that the risk of secondary symptomatic intracranial hemorrhage (SICH) may be increased after thrombolytic therapy in ischemic stroke patients who have cerebral microbleeds (CMBs) on T2*-weighted magnetic resonance imaging. Because of this concern, some centers withhold potentially beneficial thrombolytic therapy from these patients.

Methods—We analyzed magnetic resonance imaging data acquired within 6 hours after symptom onset from 570 ischemic stroke patients treated with intravenous tissue plasminogen activator in 13 centers in Europe, North America, and Asia. Baseline T2*-weighted magnetic resonance images were evaluated for the presence of CMBs. The primary end point was SICH, defined as clinical deterioration with an increase in the National Institutes of Health Stroke Scale score by ≥ 4 points, temporally related to a parenchymal hematoma on follow-up-imaging.

Results—A total of 242 CMBs were detected in 86 of 570 patients (15.1%). The number of CMBs ranged from 1 to 77 in the individual patient, with ≥ 5 CMBs in 6 of 570 patients (1.1%). Proportions of patients with SICH were 5.8% (95% CI, 1.9 to 13.0) in the presence of CMBs and 2.7% (95% CI, 1.4 to 4.5) in patients without CMBs ($P=0.170$, Fisher's exact test), resulting in no significant absolute increase in the risk of SICH of 3.1% (95% CI, -2.0 to 8.3).

Conclusions—The data suggest that if there is any increased risk of SICH attributable to CMBs, it is likely to be small and unlikely to exceed the benefits of thrombolytic therapy. No reliable conclusion regarding risk in the rare patient with multiple CMBs can be reached. (*Stroke*. 2007;38:000-000.)

Fiehler J et al. Stroke 2007;38: 2738-44.

Validació, Qualificació Volum Infart

Clinical Investigative Study

Reliability of the ABC/2 Method in Determining Acute Infarct Volume

Salvador Pedraza, MD, Josep Puig, MD, Gerard Blasco, BSc, Josep Daunis-i-Estadella, PhD, Imma Boada, PhD, Anton Bardera, PhD, Mar Castellanos, MD, PhD, Joaquín Serena, MD, PhD

From the Department of Radiology (IDI), Girona Biomedical Research Institute (IDIBGI), Hospital Universitari de Girona Dr Josep Trueta, Universitat de Girona, Girona, Spain (SP, JP, GB); and Department of Informatics and Applied Mathematics, Universitat de Girona (JDE), Institut d'Informàtica i Aplicacions, Universitat de Girona (IB, AB), Department of Neurology, Hospital Universitari Dr Josep Trueta (MC, JS), Programa de Doctorat, Departament de Medicina, Universitat Autònoma de Barcelona, Barcelona, Spain (SP).

Pedraza S et al. Reliability of the ABC/2 Method in determining Acute infarct Volume.. J Neuroimaging 2011.

Reliability of the ABC/2 Method in Determining Acute Infarct Volume

Salvador Pedraza, MD, Josep Puig, MD, Gerard Blasco, BSc, Josep Daunis-i-Estadella, PhD, Imma Boada, PhD, Anton Bardera, PhD, Mar Castellanos, MD, PhD, Joaquín Serena, MD, PhD

From the Department of Radiology (IDI), Girona Biomedical Research Institute (IDIBGI), Hospital Universitari de Girona Dr Josep Trueta, Universitat de Girona, Girona, Spain (SP, JP, GB); and Department of Informatics and Applied Mathematics, Universitat de Girona (JDE), Institut d'Informàtica i Aplicacions, Universitat de Girona (IB, AB), Department of Neurology, Hospital Universitari Dr Josep Trueta (MC, JS), Programa de Doctorat, Departament de Medicina, Universitat Autònoma de Barcelona, Barcelona, Spain (SP).

ABSTRACT

BACKGROUND AND PURPOSE

Infarct volume is used as a surrogate outcome measure in clinical trials of therapies for acute ischemic stroke. ABC/2 is a fast volumetric method, but its accuracy remains to be determined. We aimed to study the accuracy and reproducibility of ABC/2 in determining acute infarct volume with diffusion-weighted imaging.

METHODS

We studied 86 consecutive patients with acute ischemic stroke. Three blinded observers determined volume with the ABC/2 method, and the results were compared with those of the manual planimetric method.

RESULTS

The ABC/2 technique overestimated infarct volume by a median false increase (variable ABC/2 volume minus planimetric volume) of 7.33 cm³ (1.29, 22.170, representing a 162.56% increase over the value of the gold standard (variable ABC/2 volume over planimetric volume) (121.70, 248.52). In each method, the interrater reliability was excellent: the intraclass correlations were .992 and .985 for the ABC/2 technique and planimetric method, respectively.

CONCLUSIONS

ABC/2 is volumetric method with clinical value but it consistently overestimates the real infarct volume.

Keywords: Stroke, volume, infarct.

Acceptance: Received September 21, 2010, and in revised form November 10, 2010. Accepted for publication December 8, 2010.

Correspondence: Address correspondence to Salvador Pedraza, MD, Centro de RM, IDI, Servicio de Radiología, Hospital Universitari Dr Josep Trueta, Av de Francia sn, Girona 17007, Spain. E-mail: sapedraza@gmail.com.

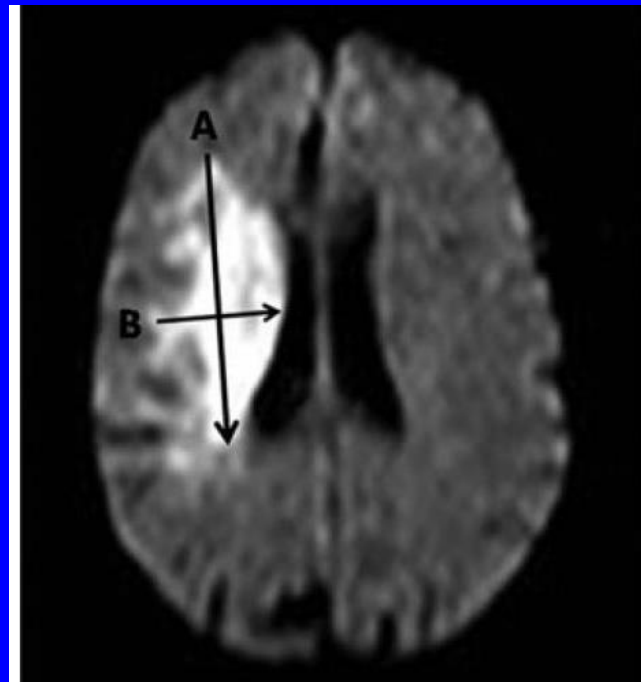
Conflict of Interest: None.

Funding: This work was supported in part by governments' grants: From MEC TIN2010-21089-C03-01 and from Fondo de Investigaciones Sanitarias (FIS) grant (reference PI09/00596).

J Neuroimaging 2011;XX:1-5
DOI: 10.1111/j.1552-6569.2011.00588.x

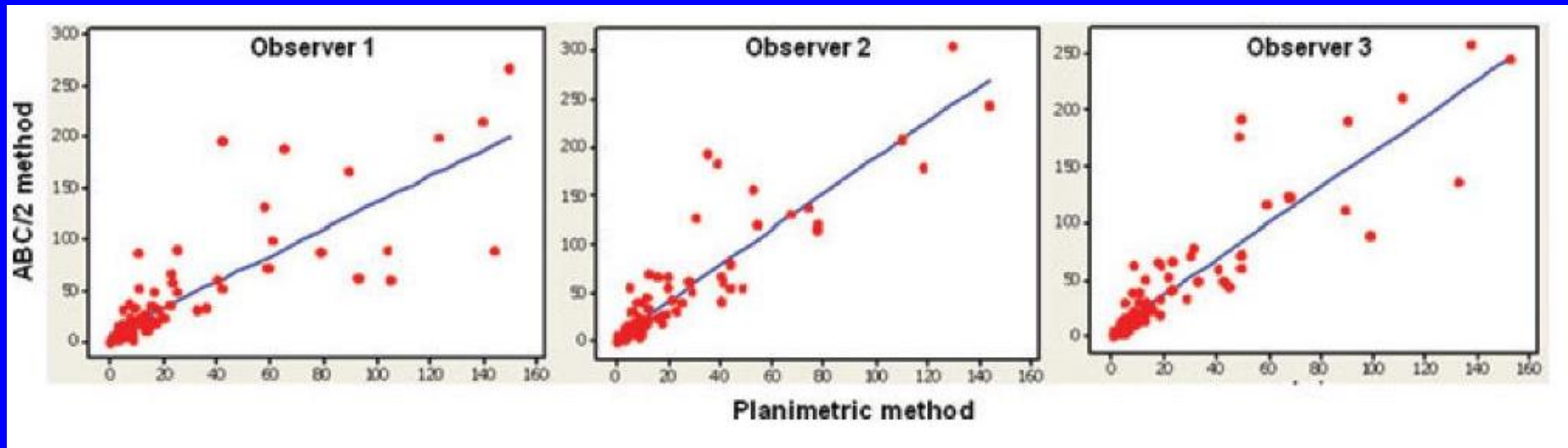
Pedraza S et al. Reliability of the ABC/2 Method in determining Acute infarct Volume.. J Neuroimaging 2011.

- .El volum d' infart es un biomarcador pronòstic important.
- .El mètode ABC/2 es un Técnica ràpida de càlcul del volum.
- .però quina es la seva validesa?



Pedraza S et al. Reliability of the ABC/2 Method in determining Acute infarct Volume.. J Neuroimaging 2011.

Bona correlació entre el volum per ABC/2 i per mètode planimètric.



Pedraza S et al. Reliability of the ABC/2 Method in determining Acute infarct Volume.. J Neuroimaging 2011.

.Hi ha diferències en el volum entre mètode ABC/2 y planimètric.
.El mètode ABC/2 exagera el volum real.

Table 2. Infarct Volume by MCA Territory in the ABC/2 and Planimetric Methods

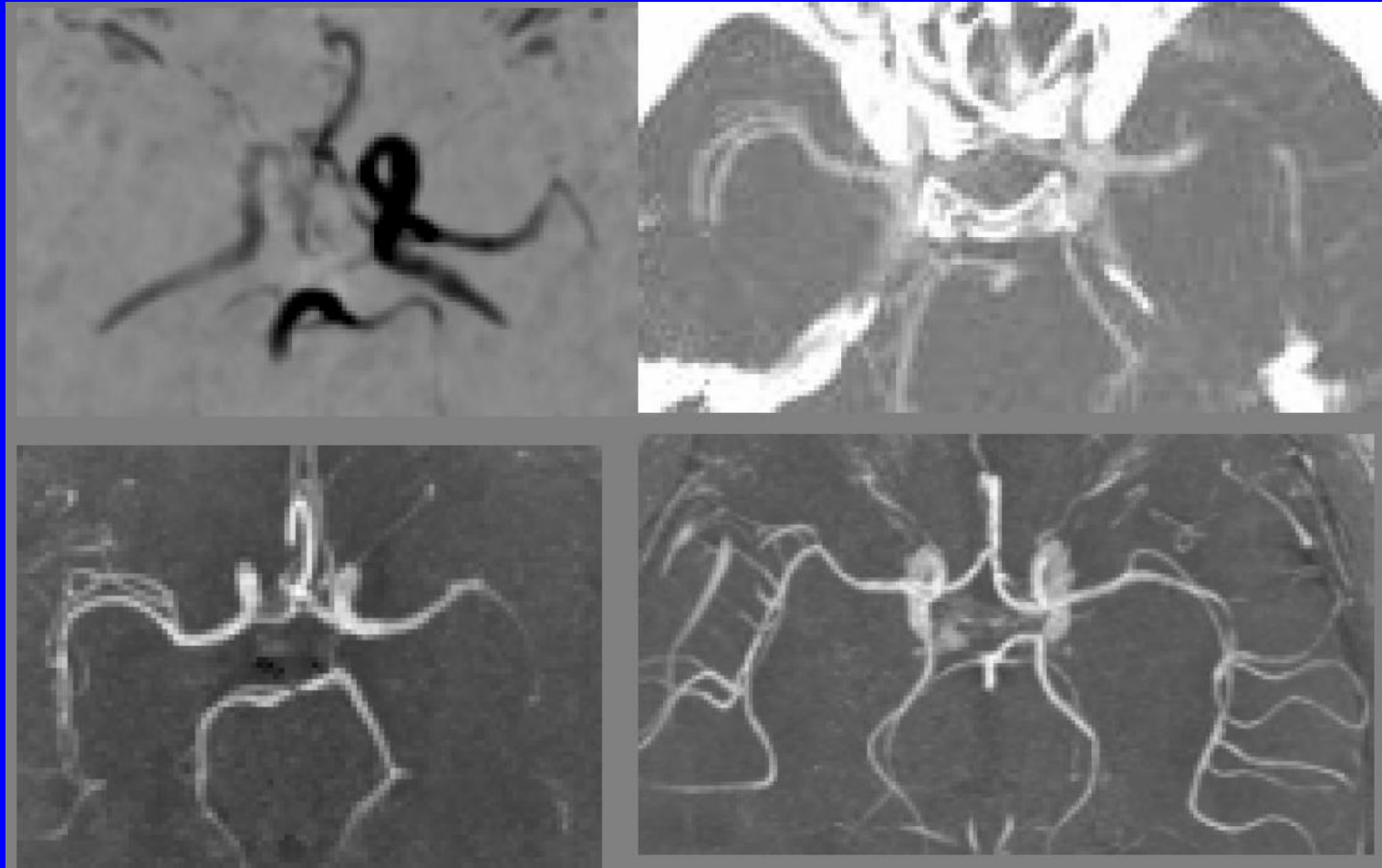
Type	ABC/2	Planimetric	Correlation	Slope	R^2
Superficial	9.04 (2.00, 15.98)	5.350 (1.88, 9.21)	.83	1.62	69.4%
Deep	21.38 (8.92, 50.64)	9.84 (5.13, 22.49)	.86	1.62	75.4%
Superficial + deep	61.2 (23.4, 130.8)	40.09 (14.93, 72.81)	.79	1.29	63.0%
Global	19.34 (8.20, 52.94)	9.93 (4.92, 23.09)	.86	1.52	75.4%

All values are in cc. Median, Q1 = 1st quartile, Q3 = 3rd quartile.

Pedraza S et al. Reliability of the ABC/2 Method in determining Acute infarct Volume.. J Neuroimaging 2011.

Validació, Qualificació Oclusió Vascular

TIMI grading in CTA & MRA



TIMI Grading:

0 = No perfusion

1 = Perfusion past the initial occlusion but no distal branch filling

2 = Perfusion and incomplete or slow distal branch filling

3 = Full perfusion with filling of all distal branches

Stroke

JOURNAL OF THE AMERICAN HEART ASSOCIATION

American Stroke
AssociationSM

A Division of American
Heart Association



Comparison of Preperfusion and Postperfusion Magnetic Resonance Angiography in Acute Stroke

Salvador Pedraza, Yolanda Silva, José Mendez, Luis Inaraja, Joana Vera, Joaquín
Serena and Antoni Dávalos

Stroke 2004;35:2105-2110; originally published online Jul 22, 2004;

DOI: 10.1161/01.STR.0000136950.63209.49

Stroke is published by the American Heart Association, 7272 Greenville Avenue, Dallas, TX 75214

Copyright © 2004 American Heart Association. All rights reserved. Print ISSN: 0039-2499. Online

ISSN: 1524-4628

ARM postcontraste valora millor el flux real y evita sobreestimar una oclusió arterial



Pedraza S et al. Comparison of preperfusion MRA in acute stroke. Stroke 2004; 35:2105-2110.

TABLE 1. Concordance Preperfusion MRA and Postperfusion MRA in the Estimation of MCA Patency

	Postperfusion MRA		
	TIMI I	TIMI II	TIMI III
Preperfusion MRA			
TIMI I	16	9	
TIMI II		1	5

Figures represent number of patients.

defined as unimpeded perfusion of the distal vasculature, regardless

Pedraza S et al. Comparison of preperfusion MRA in acute stroke. Stroke 2004; 35:2105-2110

Comparison of Preperfusion and Postperfusion Magnetic Resonance Angiography in Acute Stroke

Salvador Pedraza, MD; Yolanda Silva, MD; José Mendez, MD; Luis Inaraja, MD, PhD;
Joana Vera, MD; Joaquín Serena, MD, PhD; Antoni Dávalos, MD, PhD

Background and Purpose—The multimodal magnetic resonance imaging study in acute stroke includes perfusion-weighted imaging (PWI) after administration of contrast and magnetic resonance angiography (MRA). However, MRA may overestimate the degree of vessel obstruction caused by limitations to detect low flow states. Our aim was to determine the usefulness of a new fast imaging protocol combining classical MRA, PWI, and postperfusion MRA to improve the diagnostic management in acute ischemic stroke.

Methods—We studied 31 patients with a middle cerebral artery (MCA) infarction within the first 12 hours from the onset of symptoms. All patients had an MCA stenosis or occlusion. The study protocol included a preperfusion MRA and a postperfusion MRA. Modified thrombolysis in myocardial infarction (TIMI) classification was used to assess the patency of vessels.

Results—In 17 patients (group A, 55%), preperfusion MRA and postperfusion MRA accorded in the estimation of vascular status, whereas in 14 patients (group B, 45%) postperfusion MRA showed a better vascular flow than preperfusion MRA. The improvement in the depiction of flow was from a complete occlusion (TIMI I) to a partial occlusion (TIMI II) in 9 patients and from TIMI II to normal patency (TIMI III) in 5 patients. Thirty-six percent of the patients with suspected internal carotid artery occlusion in the preperfusion MRA showed flow in the intracranial internal carotid artery in the postperfusion MRA.

Conclusions—Postperfusion contrast-enhanced MRA can demonstrate arterial segments with low flow and avoid overestimation of vascular obstruction. (*Stroke*. 2004;35:2105-2110.)

Key Words: angiography ■ contrast media ■ magnetic resonance ■ myocardial infarction

Pedraza S et al. Comparison of preperfusion MRA in acute stroke. Stroke 2004; 35:2105-2110

Stroke

JOURNAL OF THE AMERICAN HEART ASSOCIATION



Vascular Occlusion Enables Selecting Acute Ischemic Stroke Patients for Treatment With Desmoteplase

Jochen B. Fiebach, Yasir Al-Rawi, Max Wintermark, Anthony J. Furlan, Howard A. Rowley, Annika Lindstén, Jamal Smyej, Paul Eng, Steven Warach and Salvador Pedraza

Stroke. 2012;43:1561-1566; originally published online April 3, 2012;

doi: 10.1161/STROKEAHA.111.642322

Stroke is published by the American Heart Association, 7272 Greenville Avenue, Dallas, TX 75231

Copyright © 2012 American Heart Association, Inc. All rights reserved.

Print ISSN: 0039-2499. Online ISSN: 1524-4628

Vascular Occlusion Enables Selecting Acute Ischemic Stroke Patients for Treatment With Desmoteplase

Jochen B. Fiebach, MD; Yasir Al-Rawi, MBChB; Max Wintermark, MD; Anthony J. Furlan, MD;
Howard A. Rowley, MD; Annika Lindstén, BSc; Jamal Smyej, BSc; Paul Eng, PhD;
Steven Warach, MD; Salvador Pedraza, MD

Background and Purpose—Desmoteplase is a novel and highly fibrin-specific thrombolytic agent. Evidence of safety and efficacy was obtained in 2 phase II trials (Desmoteplase In Acute Ischemic Stroke [DIAS] and Desmoteplase for Acute Ischemic Stroke [DEDAS]). The DIAS-2 phase III trial did not replicate the positive phase II efficacy findings. Post hoc analyses were performed with the aim of predicting treatment responders based on CTA and MRA.

Methods—Patients were grouped according to vessel status (Thrombolysis In Myocardial Infarction [TIMI] grade) for logistic regression of clinical response, applying the data from DIAS-2 as well as the pooled data from DIAS, DEDAS, and DIAS-2.

Results—In DIAS-2, a substantial number of mismatch-selected patients (126/179; 70%) presented with a normal flow/low-grade stenosis (TIMI 2–3) at screening, with the majority having a favorable outcome at day 90. In contrast, favorable outcome rates in patients with vessel occlusion/high-grade stenosis (TIMI 0–1) were 18% with placebo versus 36% and 27% with desmoteplase 90 and 125 $\mu\text{g/kg}$, respectively. The clinical effect based on the pooled data from DIAS, DEDAS, and DIAS-2 was favorable for desmoteplase-treated patients presenting with TIMI 0 to 1 at baseline (OR, 4.144; 95% CI, 1.40–12.23; $P=0.010$). There was no desmoteplase treatment benefit in patients presenting with TIMI 2 to 3 (OR, 1.109).

Conclusions—In this sample of patients with a mismatch diagnosed, proximal vessel occlusion or severe stenosis was associated with clinically beneficial treatment effects of desmoteplase. Selecting patients using CTA or MRA in clinical trials of thrombolytic therapy is justifiable.

Clinical Trial Registration Information—URL: <http://www.clinicaltrials.gov>. Unique identifiers: NCT00638781, NCT00638248, NCT00111852.

(Stroke. 2012;43:00-00.)

Key Words: computed tomography angiography ■ desmoteplase ■ magnetic resonance angiography ■ occlusion
■ stroke



Resultats

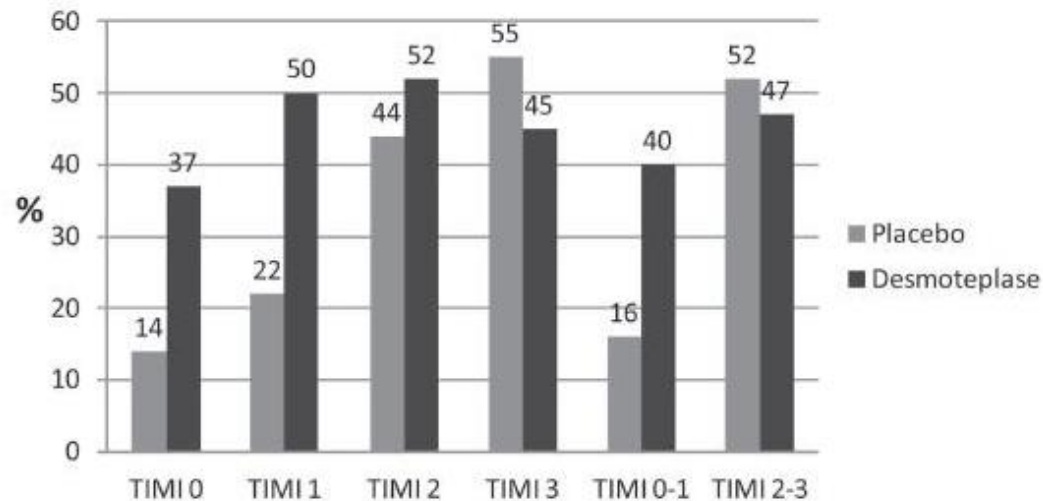


Figure 1. Composite outcome (National Institutes of Health Stroke Scale [NIHSS], modified Rankin Scale, Barthel Index) by Thrombolysis In Myocardial Infarction (TIMI) grade (pooled Desmoteplase In Acute Ischemic Stroke [DIAS] and Desmoteplase for Acute Ischemic Stroke [DEDAS], and DIAS-2 data).

Resultats

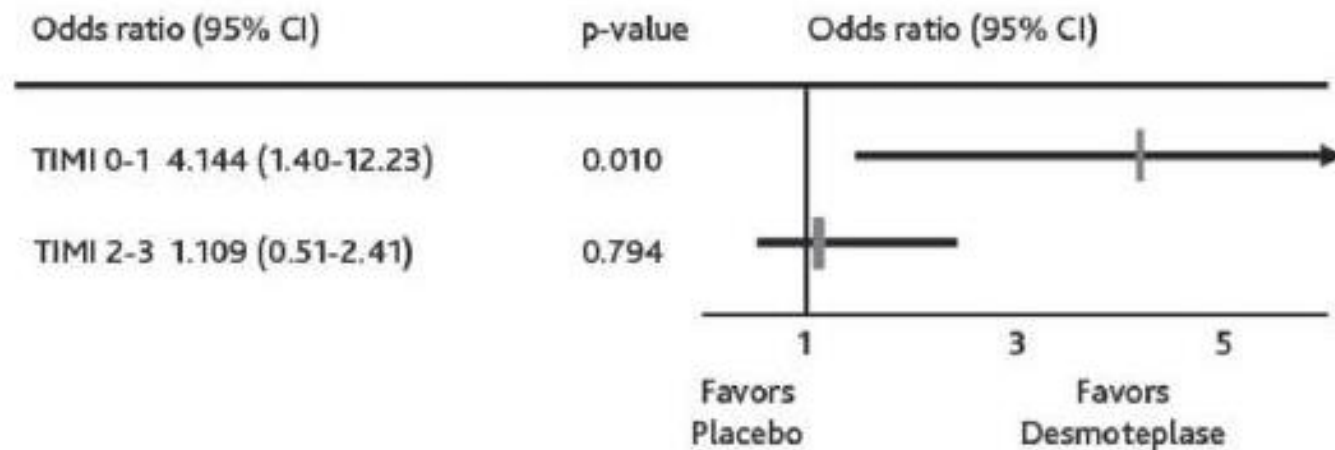


Figure 2. Favorable outcome at day 90 for Thrombolysis In Myocardial Infarction (TIMI) 0 to 1 and TIMI 2 to 3 subgroups (pooled analysis Desmoteplase In Acute Ischemic Stroke [DIAS] and Desmoteplase for Acute Ischemic Stroke [DEDAS], and DIAS-2 data).

Valor de oclusió vascular

En aquest grup de malalts amb mismatch

La oclusió o estenosis severa arterial proximal s'associava a una milloria clínica amb el tractament.

Validació, Qualificació Perfusió

Stroke

JOURNAL OF THE AMERICAN HEART ASSOCIATION



American
Heart
Association | American
Stroke
Association®

Comparative Overview of Brain Perfusion Imaging Techniques

Max Wintermark, Musa Sesay, Emmanuel Barbier, Katalin Borbély, William P. Dillon, James D. Eastwood, Thomas C. Glenn, Cécile B. Grandin, Salvador Pedraza, Jean-François Soustiel, Tadashi Nariai, Greg Zaharchuk, Jean-Marie Caillé, Vincent Dousset and Howard Yonas

Stroke. 2005;36:e83-e99; originally published online August 11, 2005;

doi: 10.1161/01.STR.0000177884.72657.8b

Stroke is published by the American Heart Association, 7272 Greenville Avenue, Dallas, TX 75231

Copyright © 2005 American Heart Association, Inc. All rights reserved.

Print ISSN: 0039-2499. Online ISSN: 1524-4628

TABLE 1. Overview of the Imaging Techniques Dedicated to Brain Hemodynamics

	Brain Perfusion Imaging Techniques						
	PET	SPECT	XeCT	PCT	DSC	ASL	Doppler
Feasibility							
Age range	Adults (and children for static exams)	Adults (and children)	Adults (and children)	Adults (and children)	Adults (and children)	Adults+children	Adults+children
Bedside	No	In some instances	No	No	No	No	Yes
Contrast material	$^{15}\text{O}_2$, C^{18}O_2 , H_2^{15}O	^{133}Xe , $^{99\text{m}}\text{Tc-HMPAO}$, $^{99\text{m}}\text{Tc-ECD}$, $^{123}\text{I-IMP}$ (diffusible)	Stable xenon gas (diffusible)	Iodinated contrast material (nondiffusible)	gadolinium chelate (nondiffusible)	None (endogenous contrast)	None (endogenous contrast)
Radiation/study	0.5–2 mSv	3.5–12 mSv	3.5–10 mSv	2–3 mSv	None	None	None
Data acquisition	5–9 min	10–15 min	10 min	40 sec	1 min	5–10 min	10–20 min
Data processing	5–10 min	5 min	10 min	5 min	5 min	5 min	None
Interpretation							
Mathematical model	Kety–Schmidt model	Principle of chemical microspheres for $^{99\text{m}}\text{Tc}$ tracers, Kety–Schmidt model for ^{133}Xe and $^{123}\text{I-IMP}$	Kety–Schmidt model	Meier–Zierler model	Meier–Zierler model	Meier–Zierler model	Other
Assessed parameters	CBV, CBF, rOEF, glucose metabolism	CBF	CBF	CBF, CBV, MTT, TTP, permeability map	CBF, CBV, MTT, TTP, permeability map	CBF	ICA BFV
Large vessels*	No influence on results	No influence on results	No influence on results	Influence results	Influence results	No influence on results	Not applicable
Quantitative accuracy	Yes	Yes for ^{133}Xe and $^{123}\text{I-IMP}$; no for the others tracers	Yes	Yes	Not in daily practice	Yes	Yes for hemispheric CBF
Including for low perfused areas†	Yes	Not applicable	Yes	Yes	Not applicable	Not <10 mL/min/100 g	Not applicable
Reproducibility	5%	10%	12%	10–15%	10–15%	10%	5%
Brain coverage	Whole brain	Whole brain	6-cm thickness	4–5 cm thickness	Whole brain	Whole brain	One measurement for each hemisphere
Spatial resolution	4–6 mm	4–6 mm	4 mm	1–2 mm	2 mm	2 mm	Not applicable
Minimal time interval between 2 successive exams	10 min	10 min (split-dose technique for $^{99\text{m}}\text{Tc-HMPAO}$, $^{99\text{m}}\text{Tc-ECD}$ and $^{123}\text{I-IMP}$)	20 min	10 min	25 min	0 min	0 min
Clinical applications							
Clinical fields	Chronic cerebrovascular disorders	(Acute and) chronic cerebrovascular disorders	Acute and chronic cerebrovascular disorders	Acute and chronic cerebrovascular disorders	Acute and chronic cerebrovascular disorders	Chronic cerebrovascular disorders	Acute cerebrovascular disorders
		Trauma	Trauma	Trauma		Trauma	Trauma
	Dementia and psychiatric diseases	Dementia and psychiatric diseases	Vasospasm	Vasospasm	Vasospasm	Neurodegenerative disorders	Vasospasm
	Epilepsy	Epilepsy	Epilepsy				
	Brain tumors			Brain tumors	Brain tumors	Brain tumors	
	Brain activation studies	Brain activation studies				Brain activation studies	
Emergency setting	No	In some instances	Yes	Yes	Yes	Yes	Yes

Wintermark M et al. Stroke 2005; 2005;36:e83-e99.

TABLE 2. Main Strengths and Weaknesses of the Imaging Techniques Dedicated to Brain Hemodynamics

	Brain Perfusion Imaging Techniques						
	PET	SPECT	XeCT	PCT	DSC	ASL	Doppler
Main strengths	Accurate quantitative measurements	Technetium generator widely available	Accurate quantitative measurements	Wide availability of necessary equipment, including in the emergency setting	Can be combined with fine anatomic imaging, DWI, MRA, spectroscopy, providing the most comprehensive information in one examination	Repeatability (attributable to a lack of ionizing radiation)	Can be performed at bedside
	Assessment of multiple factors using various radioligands	Can be used at bedside and in the emergency setting	Assessment of multiple brain levels	Access to multiple perfusion parameters (CBV, CBF, MTT)	Repeatability (attributable to a lack of ionizing radiation)	Noninvasiveness (no intravenous injections)	Repeatability (attributable to a lack of ionizing radiation)
	Repeated measurements possibly attributable to short half-life of radiotracers	Low cost	Can be repeated at 10-minute intervals providing an ability to measure the CBF response to interventions	Accurate quantitative measurements	Whole brain coverage	flexibility (spatial resolution and imaging time can be traded off depending on the clinical question)	Noninvasiveness (no intravenous injections)
Main weaknesses	Impossible to use in the emergency settings	Relative, not quantitative measurements	Relatively long acquisition time, prone to motion artifacts	Presently limited anatomic coverage	Lack of standardization in the interpretation	CBF underestimation associated with extremely delayed arterial arrival times (such as through collateral pathways)	Provides only one value for each brain hemisphere
	High cost (however, cost-effective in well-established diagnostic algorithms)	Poor spatial resolution	Inhalation of Xenon via a face mask	use of ionizing radiation and iodinated contrast media	Not available in the emergency settings in most institutions	Relatively low signal-to-noise ratio per unit time	Operator dependent
			Xenon not currently approved by the FDA (technology only available at this time under IND status)		Difficulties associated with obtaining MRI (claustrophobia, contraindications, and access issues)	Difficulties associated with obtaining MRI (claustrophobia, contraindications, and access issues)	

Wintermark M et al. Stroke 2005; 2005;36:e83-e99.

Validació, Qualificació Perfusió CT

Stroke

JOURNAL OF THE AMERICAN HEART ASSOCIATION

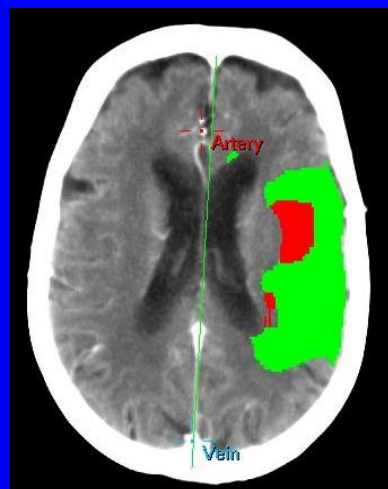


American Heart Association | American Stroke Association

Perfusion-CT Assessment of Infarct Core and Penumbra : Receiver Operating Characteristic Curve Analysis in 130 Patients Suspected of Acute Hemispheric Stroke
Max Wintermark, Adam E. Flanders, Birgitta Velthuis, Reto Meuli, Maarten van Leeuwen, Dorit Goldsher, Carissa Pineda, Joaquin Serena, Irene van der Schaaf, Annet Waaijer, James Anderson, Gary Nesbit, Igal Gabriely, Victoria Medina, Ana Quiles, Scott Pohlman, Marcel Quist, Pierre Schnyder, Julien Bogousslavsky, William P. Dillon and Salvador Pedraza

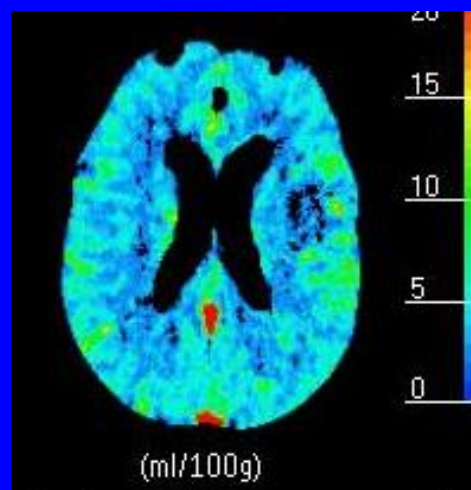
Stroke. 2006;37:979-985; originally published online March 2, 2006;
doi: 10.1161/01.STR.0000209238.61459.39

Stroke is published by the American Heart Association, 7272 Greenville Avenue, Dallas, TX 75231
Copyright © 2006 American Heart Association, Inc. All rights reserved.
Print ISSN: 0039-2499. Online ISSN: 1524-4628

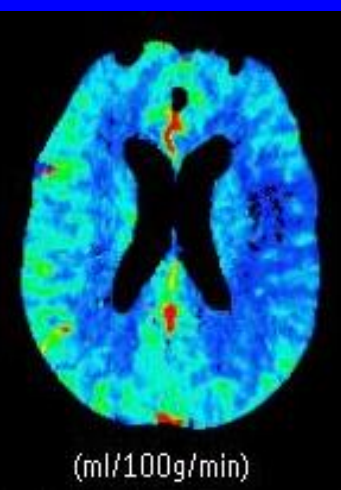


Summary map

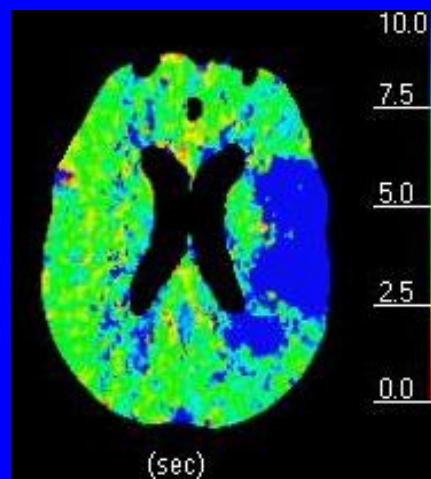
CBV



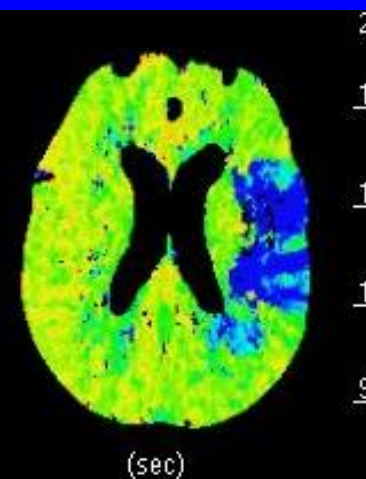
CBF



MTT



TTP



$$\text{CBV} = 2.0 \text{ ml} \times 100 \text{ g.}$$

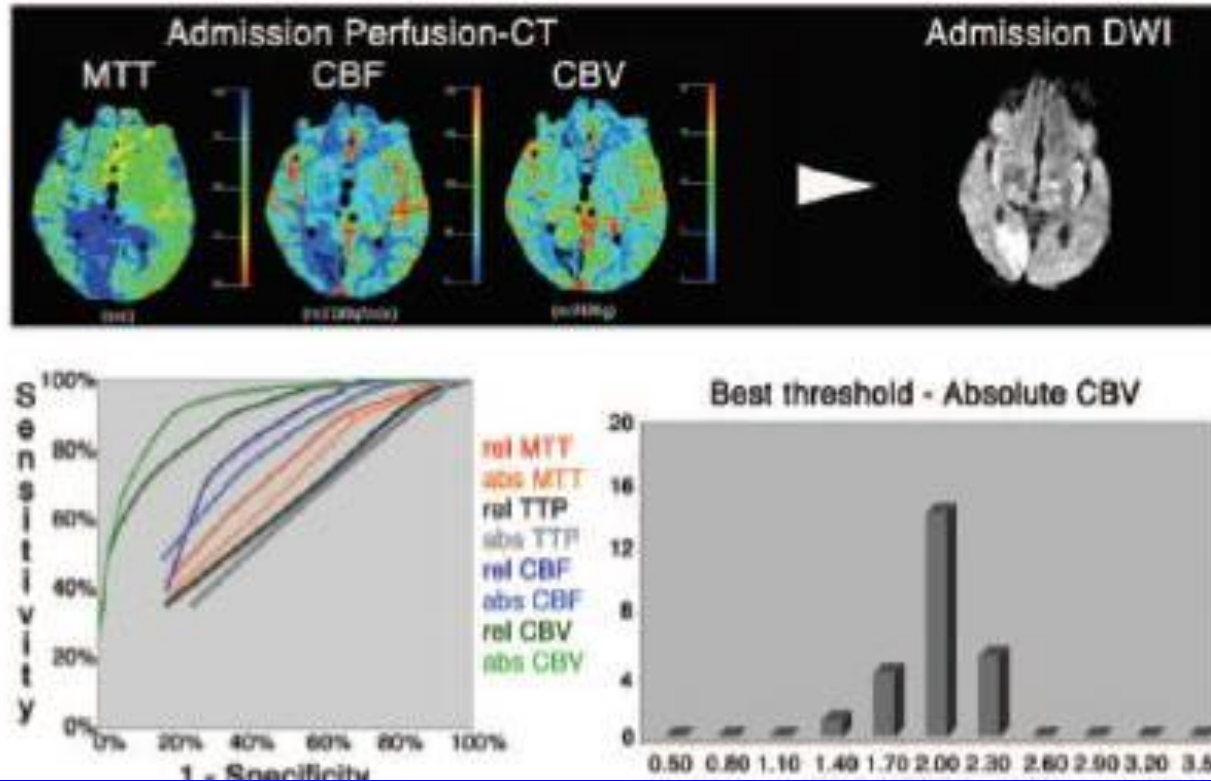


Figure 2. ROC analysis in the 25 patients of Group D, who underwent admission DWI (total of 5 911 234 pixels). The PCT parameter most accurately predicting the acute infarct volume on the admission DWI study is the absolute CBV (AUC=0.927). The optimal threshold for absolute CBV is $2.0 \text{ ml} \times 100 \text{ g}^{-1}$. The histogram (Inferior right) of the best thresholds obtained by the ROC analysis performed separately for each patient (considering all pixels in each patient) reveals a narrow distribution around the value of $2.0 \text{ ml} \times 100 \text{ g}^{-1}$ obtained with the global analysis (Inferior left).

Wintermark M et al. Stroke 2005;37:979-985.

MTT: 145%

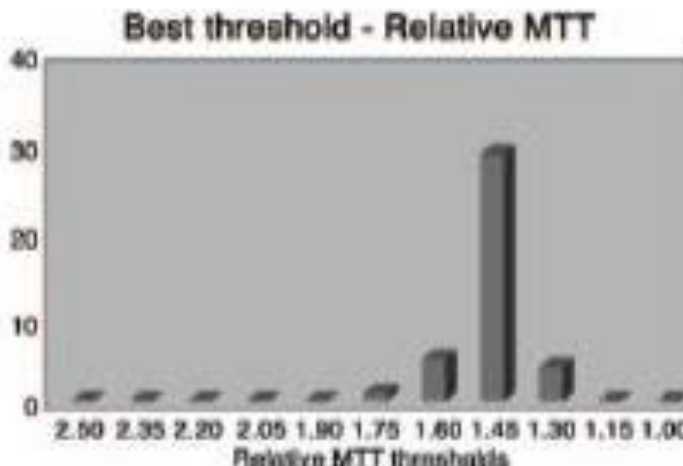
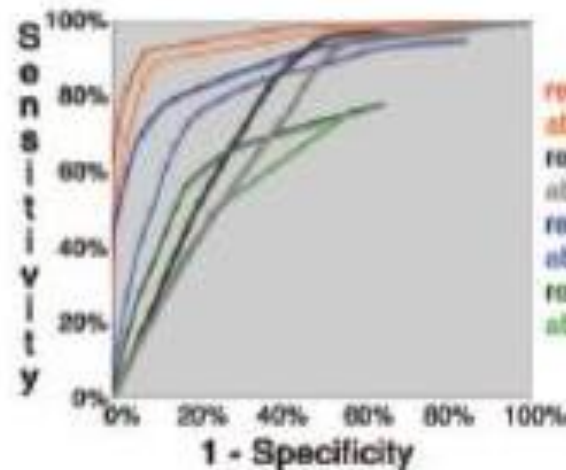
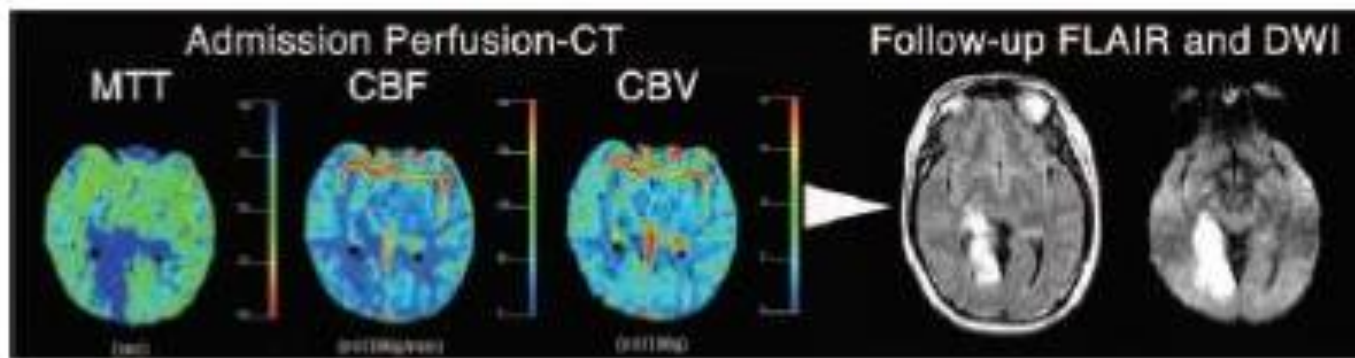


Figure 1. ROC curve analysis in the 46 patients of Group A, showing persistent arterial occlusion on the follow-up MRA (total of 11 817 345 pixels). The PCT parameter most accurately predicting the issue at risk of infarction on the follow-up MRI study (FLAIR and DWI used as references) is the relative MTT (AUC=0.962). The optimal threshold for relative MTT is 145%. The histogram (inferior right) of the best thresholds obtained by the ROC analysis performed separately for each patient (considering all pixels in each patient) reveals a narrow distribution around the value of 45% obtained with the global analysis (inferior left).

Wintermark M et al. Stroke 2005;37:979-985.

**Validació,
Qualificació
Penumbra
RM i TC**

Intravenous desmoteplase in patients with acute ischaemic stroke selected by MRI perfusion–diffusion weighted imaging or perfusion CT (DIAS-2): a prospective, randomised, double-blind, placebo-controlled study

Werner Hacke, Anthony J Furlan, Yasir Al-Rawi, Antoni Davalos, Jochen B Fiebach, Franz Gruber, Markku Kaste, Leslie J Lipka, Salvador Pedraza, Peter A Ringleb, Howard A Rowley, Dietmar Schneider, Lee H Schwamm, Joaquin Serena Leal, Mariola Söhngen, Phil A Teal, Karin Wilhelm-Ogunbiyi, Max Wintermark, Steven Warach

Hacke W et al. Lancet Neurol. 2009 Feb;8(2):141-50.

	Desmoteplase 90 µg/kg (n=57)	Desmoteplase 125 µg/kg (n=66)	Placebo (n=63)	p value (global test)
Composite responder rate	27 (47%)	24 (36%)	29 (46%)	0.47
Individual component responder rate				
NIHSS ≤1 or improvement ≥8 points	33 (58%)	33 (50%)	37 (59%)	..
mRS score 0-2	31 (54%)	32 (49%)	36 (57%)	..
Barthel index 75-100	39 (68%)	36 (55%)	42 (67%)	..

NIHSS=National Institutes of Health stroke scale. mRS=modified Rankin scale.

Table 2: Primary efficacy endpoint (composite responder rate at day 90) in the intention-to-treat population

Hacke W et al. Lancet Neurol. 2009 Feb;8(2):141-50.

Intravenous desmoteplase in patients with acute ischaemic stroke selected by MRI perfusion-diffusion weighted imaging or perfusion CT (DIAS-2): a prospective, randomised, double-blind, placebo-controlled study

Werner Hacke, Anthony J Furlan, Yasir Al-Rawi, Antoni Davalos, Jochen B Fiebach, Franz Gruber, Markku Kaste, Leslie J Lipka, Salvador Pedraza, Peter A Ringleb, Howard A Rowley, Dietmar Schneider, Lee H Schwamm, Joaquin Serena Leal, Mariola Söhlngen, Phil A Teal, Karin Wilhelm-Ogunbiyi, Max Wintermark, Steven Warach

Summary

Background Previous studies have suggested that desmoteplase, a novel plasminogen activator, has clinical benefit when given 3–9 h after the onset of the symptoms of stroke in patients with presumptive tissue at risk that is identified by magnetic resonance perfusion imaging (PI) and diffusion-weighted imaging (DWI).

Methods In this randomised, placebo-controlled, double-blind, dose-ranging study, patients with acute ischaemic stroke and tissue at risk seen on either MRI or CT imaging were randomly assigned (1:1:1) to 90 µg/kg desmoteplase, 125 µg/kg desmoteplase, or placebo within 3–9 h after the onset of symptoms of stroke. The primary endpoint was clinical response rates at day 90, defined as a composite of improvement in National Institutes of Health stroke scale (NIHSS) score of 8 points or more or an NIHSS score of 1 point or less, a modified Rankin scale score of 0–2 points, and a Barthel index of 75–100. Secondary endpoints included change in lesion volume between baseline and day 30, rates of symptomatic intracranial haemorrhage, and mortality rates. Analysis was by intention to treat. This study is registered with ClinicalTrials.gov, NCT00111852.

Findings Between June, 2005, and March, 2007, 193 patients were randomised, and 186 patients received treatment: 57 received 90 µg/kg desmoteplase; 66 received 125 µg/kg desmoteplase; and 63 received placebo. 158 patients completed the study. The median baseline NIHSS score was 9 (IQR 6–14) points, and 30% (53 of 179) of the patients had a visible occlusion of a vessel at presentation. The core lesion and the mismatch volumes were small (median volumes were 10.6 cm³ and 52.5 cm³, respectively). The clinical response rates at day 90 were 47% (27 of 57) for 90 µg/kg desmoteplase, 36% (24 of 66) for 125 µg/kg desmoteplase, and 46% (29 of 63) for placebo. The median changes in lesion volume were: 90 µg/kg desmoteplase 14.0% (0.5 cm³); 125 µg/kg desmoteplase 10.8% (0.3 cm³); placebo –10.0% (–0.9 cm³). The rates of symptomatic intracranial haemorrhage were 3.5% (2 of 57) for 90 µg/kg desmoteplase, 4.5% (3 of 66) for 125 µg/kg desmoteplase, and 0% for placebo. The overall mortality rate was 11% (5% [3 of 57] for 90 µg/kg desmoteplase; 21% [14 of 66] for 125 µg/kg desmoteplase; and 6% [4 of 63] for placebo).

Interpretation The DIAS-2 study did not show a benefit of desmoteplase given 3–9 h after the onset of stroke. The high response rate in the placebo group could be explained by the mild strokes recorded (low baseline NIHSS scores, small core lesions, and small mismatch volumes that were associated with no vessel occlusions), which possibly reduced the potential to detect any effect of desmoteplase.

Stroke

JOURNAL OF THE AMERICAN HEART ASSOCIATION



Refinement of the Magnetic Resonance Diffusion-Perfusion Mismatch Concept for Thrombolytic Patient Selection : Insights From the Desmoteplase in Acute Stroke Trials

Steven Warach, Yasir Al-Rawi, Anthony J. Furlan, Jochen B. Fiebach, Max Wintermark, Annika Lindstén, Jamal Smyej, David B. Bharucha, Salvador Pedraza and Howard A. Rowley

Stroke. 2012;43:2313-2318; originally published online June 26, 2012;

doi: 10.1161/STROKEAHA.111.642348

Stroke is published by the American Heart Association, 7272 Greenville Avenue, Dallas, TX 75231

Copyright © 2012 American Heart Association, Inc. All rights reserved.

Print ISSN: 0039-2499. Online ISSN: 1524-4628

Warach S et al. Stroke. 2012;43:2313-2318

Table 2. Desmoteplase Effect vs Mismatch Volume

Study	N	Baseline Mismatch Volume	Percentage of Responders		Effect Size Desmoteplase vs Placebo	OR for Responders: Desmoteplase Pooled vs Placebo
			Placebo	Pooled Desmoteplase*		
DIAS-2	122	All	45%	45%	0%	1.02 (0.47–2.21)
	45	≤60 mL	80%	63%	–17%	0.43 (0.10–1.87)
	66	>60 mL	24%	38%	14%	1.94 (0.60–6.27)
DIAS/DEDAS/ DIAS-2 (MRI)	216	All	34%	47%	13%	1.69 (0.94–3.04)
	75	≤60 mL	61%	57%	–4%	0.87 (0.34–2.27)
	117	>60 mL	21%	43%	22%	2.83 (1.16–6.94)

DEDAS indicates Dose Escalation of Desmoteplase for Acute Ischemic Stroke; DIAS, Desmoteplase In Acute Ischemic Stroke; MRI, magnetic resonance imaging; OR, odds ratio.

*90 and 125 µg/kg treatment groups.

Warach S et al. Stroke. 2012;43:2313-2318

Refinement of the Magnetic Resonance Diffusion-Perfusion Mismatch Concept for Thrombolytic Patient Selection

Insights From the Desmoteplase in Acute Stroke Trials

Steven Warach, MD, PhD; Yasir Al-Rawi, MBChB; Anthony J. Furlan, MD; Jochen B. Fiebach, MD; Max Wintermark, MD; Annika Lindstén, BSc; Jamal Smyej, BSc; David B. Bharucha, MD; Salvador Pedraza, MD; Howard A. Rowley, MD

Background and Purpose—The DIAS-2 study was the only large, randomized, intravenous, thrombolytic trial that selected patients based on the presence of ischemic penumbra. However, DIAS-2 did not confirm the positive findings of the smaller DEDAS and DIAS trials, which also used penumbral selection. Therefore, a reevaluation of the penumbra selection strategy is warranted.

Methods—In post hoc analyses we assessed the relationships of magnetic resonance imaging-measured lesion volumes with clinical measures in DIAS-2, and the relationships of the presence and size of the diffusion-perfusion mismatch with the clinical effect of desmoteplase in DIAS-2 and in pooled data from DIAS, DEDAS, and DIAS-2.

Results—In DIAS-2, lesion volumes correlated with National Institutes of Health Stroke Scale (NIHSS) at both baseline and final time points ($P < 0.0001$), and lesion growth was inversely related to good clinical outcome ($P = 0.004$). In the pooled analysis, desmoteplase was associated with 47% clinical response rate ($n = 143$) vs 34% in placebo ($n = 73$; $P = 0.08$). For both the pooled sample and for DIAS-2, increasing the minimum baseline mismatch volume (MMV) for inclusion increased the desmoteplase effect size. The odds ratio for good clinical response between desmoteplase and placebo treatment was 2.83 (95% confidence interval, 1.16–6.94; $P = 0.023$) for MMV > 60 mL. Increasing the minimum NIHSS score for inclusion did not affect treatment effect size.

Conclusions—Pooled across all desmoteplase trials, desmoteplase appears beneficial in patients with large MMV and ineffective in patients with small MMV. These results support a modified diffusion-perfusion mismatch hypothesis for patient selection in later time-window thrombolytic trials.

Clinical Trial Registration—URL: <http://www.clinicaltrials.gov>. Unique Identifiers: NCT00638781, NCT00638248, NCT00111852.

(*Stroke*. 2012;43:2313-2318.)

Key Words: acute cerebral infarction ■ desmoteplase ■ diffusion-weighted imaging ■ magnetic resonance imaging ■ mismatch ■ perfusion ■ stroke ■ thrombolysis

Warach S et al. Stroke. 2012;43:2313-2318

Validació, Qualificació Perfusió RM

A Framework to Assist Acute Stroke Diagnosis

A.Bardera *, I.Boada*, M.Feixas*, S.Pedraza[†] and J.Rodríguez*

*Institut d'Informàtica i Aplicacions, Universitat de Girona, 17071-Girona, Spain

[†] Hospital Universitari Dr. Josep Trueta, Girona, Spain

Email: {anton.bardera, imma.boada, miquel.feixas}@udg.es

**Bardera J . Proceedings of the Vision, Modeling
and Visualization 2005, Vol. 1, pp. 359-366.**



Bardera J . Proceedings of the Vision, Modeling and Visualization 2005, Vol. 1, pp. 359-366

Validació, Qualificació TC Simple

ORIGINAL
RESEARCH

J. Puig
S. Pedraza
A. Demchuk
J. Daunis-i-Estadella
H. Termes
G. Blasco
G. Soria
I. Boada
S. Remollo
J. Baños
J. Serena
M. Castellanos



Quantification of Thrombus Hounsfield Units on Noncontrast CT Predicts Stroke Subtype and Early Recanalization after Intravenous Recombinant Tissue Plasminogen Activator

BACKGROUND AND PURPOSE: Little is known about the factors that determine recanalization after intravenous thrombolysis. We assessed the value of thrombus Hounsfield unit quantification as a predictive marker of stroke subtype and MCA recanalization after intravenous rtPA treatment.

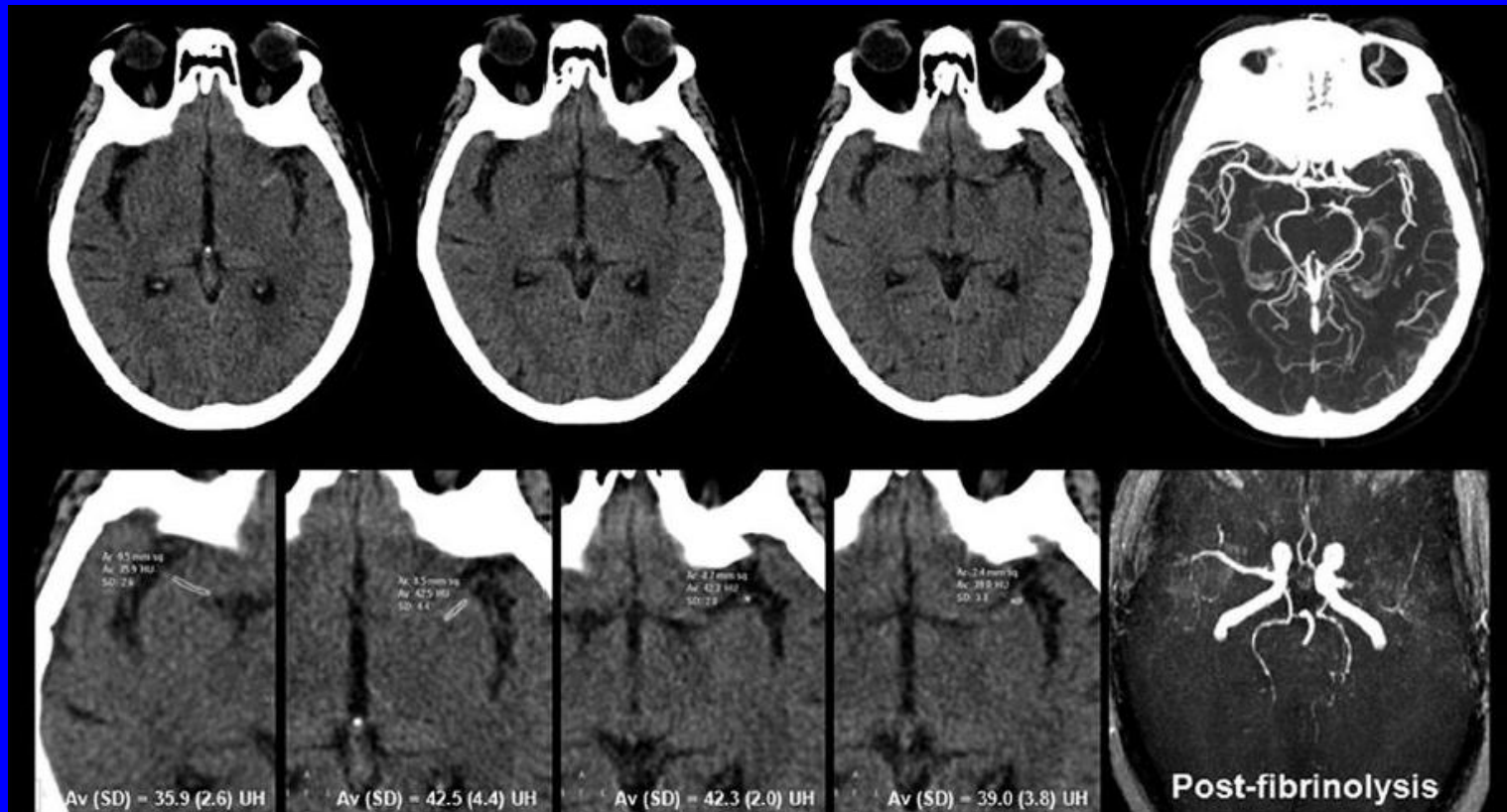
MATERIALS AND METHODS: NCCT scans and CTA were performed on patients with MCA acute stroke within 4.5 hours of symptom onset. Demographics, stroke severity, vessel hyperattenuation, occlusion site, thrombus length, and time to thrombolysis were recorded. Stroke origin was categorized as LAA, cardioembolic, or indeterminate according to TOAST criteria. Two blinded neuroradiologists calculated the Hounsfield unit values for the thrombus and contralateral MCA segment. We used ROC curves to determine the rHU cutoff point to discriminate patients with successful recanalization from those without. We assessed the accuracy (sensitivity, specificity, and positive and negative predictive values) of rHU in the prediction of recanalization.

RESULTS: Of 87 consecutive patients, 45 received intravenous rtPA and only 15 (33.3%) patients had acute recanalization. rHU values and stroke mechanism were the highest predictive factors of recanalization. The Matthews correlation coefficient was highest for rHU (0.901). The sensitivity, specificity, and positive and negative predictive values for lack of recanalization after intravenous rtPA for rHU \leq 1.382 were 100%, 86.67%, 93.75%, and 100%, respectively. LAA thrombi had lower rHU than cardioembolic and indeterminate stroke thrombi ($P = .004$).

CONCLUSIONS: The Hounsfield unit thrombus measurement ratio can predict recanalization with intravenous rtPA and may have clinical utility for endovascular treatment decision making.

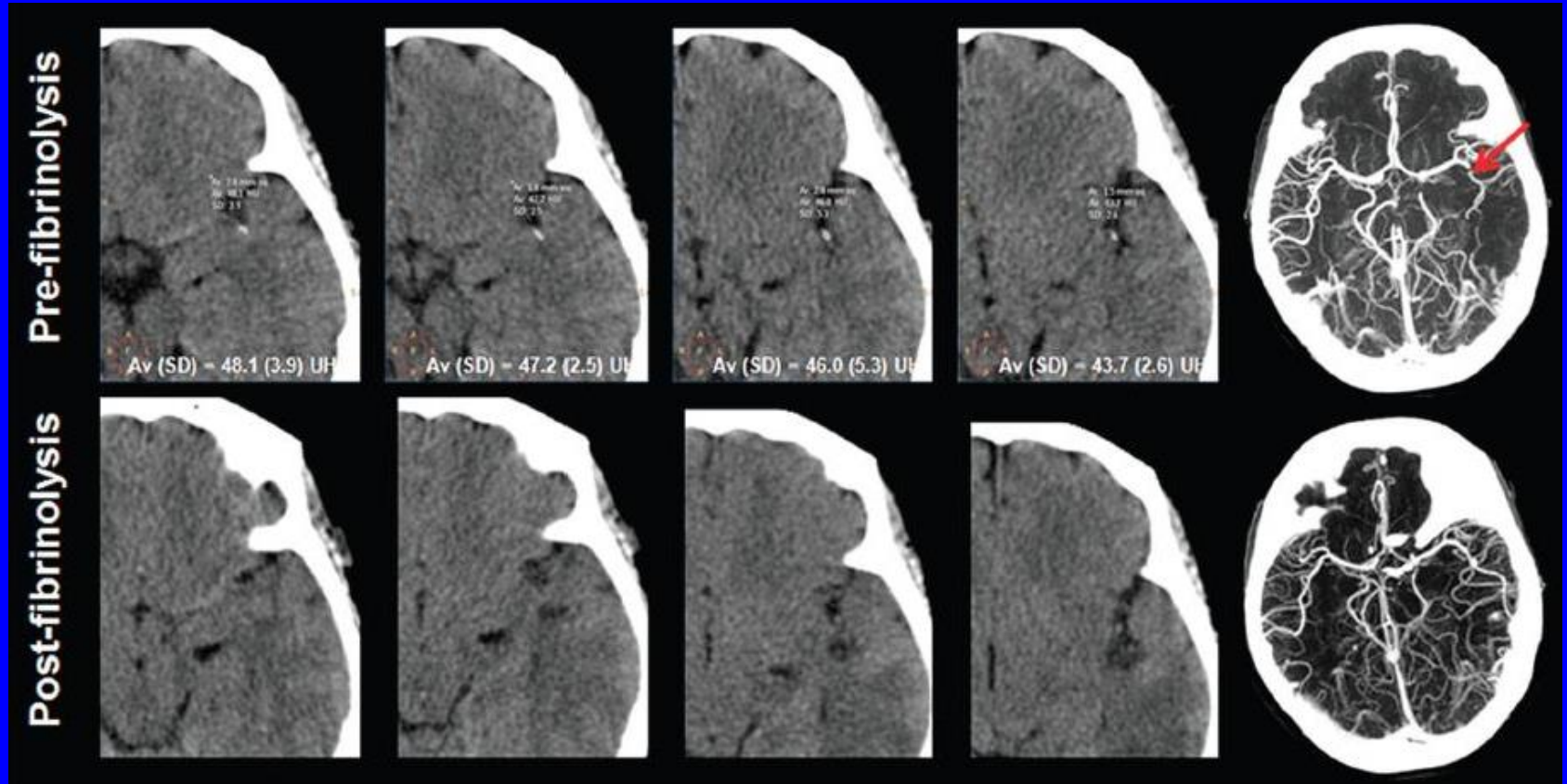
ABBREVIATIONS: ASPECTS = Alberta Stroke Program Early CT Score; DIAS = Desmoteplase in Acute Ischemic Stroke; DICOM = digital imaging and communication in medicine; HMCAS = hyperdense middle cerebral artery sign; ICC = intraclass correlation coefficient; IQR = interquartile range; LAA = large artery atherosclerosis; MIP = maximum intensity projection; mRS = modified Rankin Scale; NINDS = National Institute of Neurological Disorders and Stroke; rHU = Hounsfield Unit ratio; r_s = Matthews correlation coefficient; ROC = receiver operating characteristic; rt-PA = recombinant tissue plasminogen activator; TIBI = Thrombolysis in Brain Ischemia; TIMI = Thrombolysis in Myocardial Infarction; TOAST = Trial of Org 10172 in Acute Stroke Treatment

Ratis menors de 1.382 no recanalitza.
Pacient amb rati de 1.14 en ACM esquerra que no va recanalitza tras rTPA.



Puig J et al. Quantification of Thrombus Hounsfield Units on Noncontrast CT Predicts Stroke Subtype and Early Recanalization after Intravenous Recombinant Tissue Plasminogen. AJNR 2012.

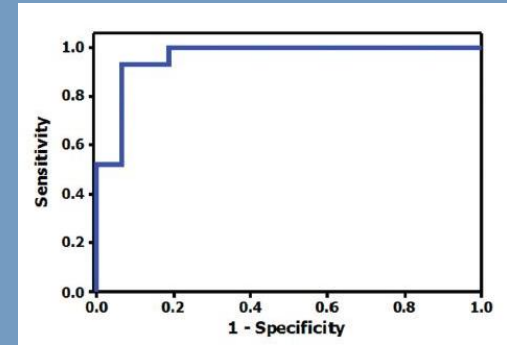
**Ratis majors de 1.382 recanalitzen.
Pacient amb rati de 1.48 en ACM esquerra que va
recanalitzar tras rTPA.**



**Puig J et al. Quantification of Thrombus Hounsfield Units on
Noncontrast CT Predicts Stroke Subtype and Early Recanalization
after Intravenous Recombinant Tissue Plasminogen. AJNR 2012.**

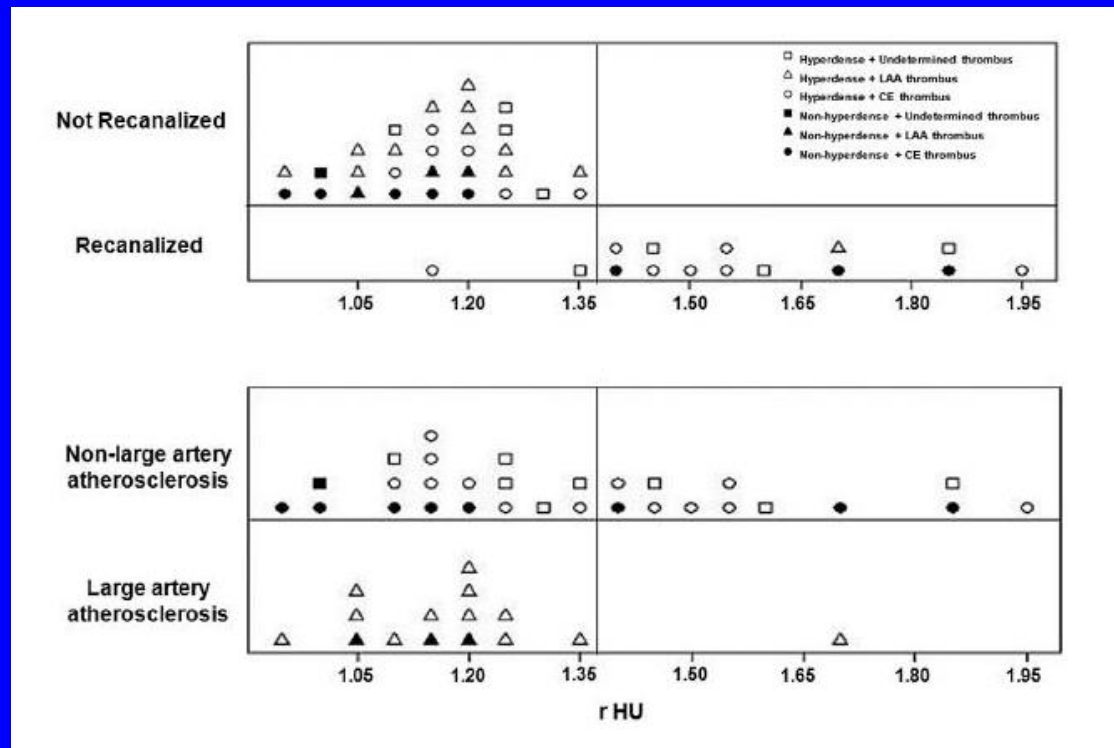
Valor per predir manca de recanalització tras rTPA de un rati menor de 1.382 ?.

- Sensibilitat: 100%
- Especificitat: 86,7%
- Valor predictiu positiu: 93.75 %
- Valor predictiu negatiu: 100%
- AUC (ROC): 0,96.



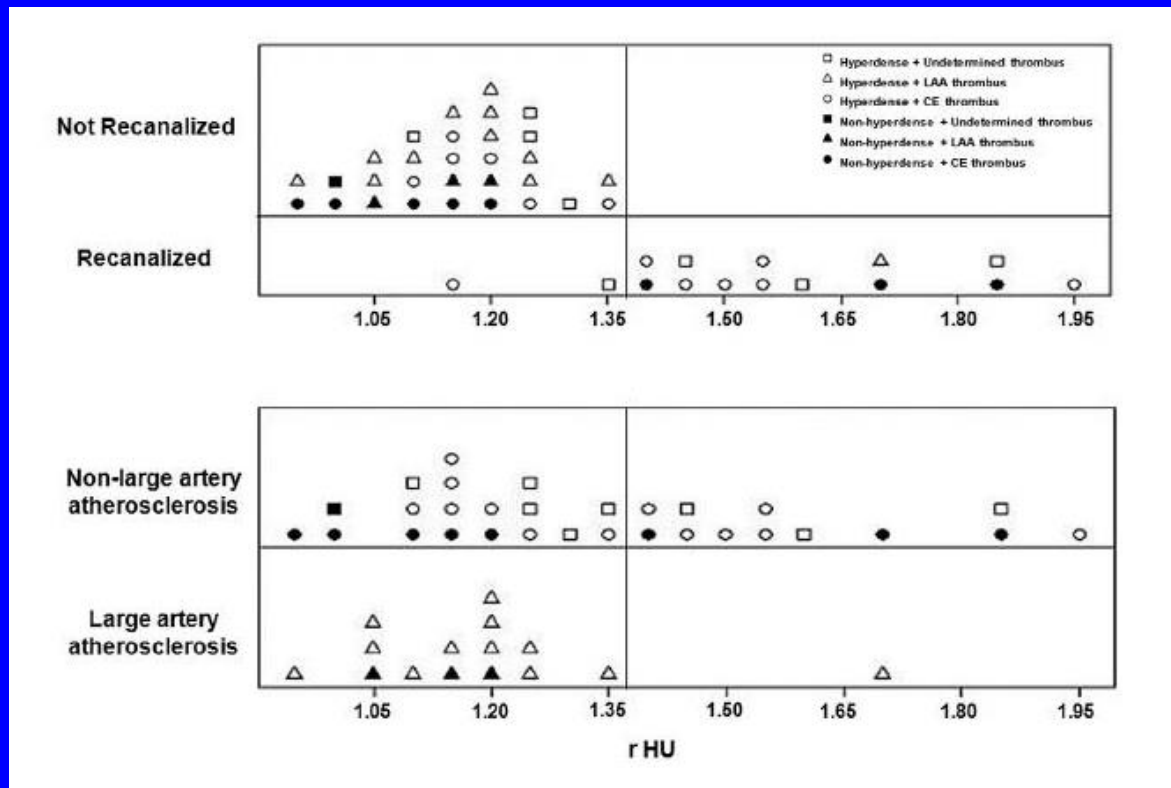
Puig J et al. Quantification of Thrombus Hounsfield Units on Noncontrast CT Predicts Stroke Subtype and Early Recanalization after Intravenous Recombinant Tissue Plasminogen. AJNR 2012.

La densitat del trombus persisteix predir la recanalització amb rTPA y pot ser útil per indicar el tractament endovascular.



Puig J et al. Quantification of Thrombus Hounsfield Units on Noncontrast CT Predicts Stroke Subtype and Early Recanalization after Intravenous Recombinant Tissue Plasminogen. AJNR 2012.

Rati >1.382 = Recanalització tras rTPA.
Rati <1.382 = No recanalització



Puig J et al. Quantification of Thrombus Hounsfield Units on Noncontrast CT Predicts Stroke Subtype and Early Recanalization after Intravenous Recombinant Tissue Plasminogen. AJNR 2012.

ORIGINAL
RESEARCH

J. Puig
S. Pedraza
A. Demchuk
J. Daunis-i-Estadella
H. Termes
G. Blasco
G. Soria
I. Boada
S. Remollo
J. Baños
J. Serena
M. Castellanos



Quantification of Thrombus Hounsfield Units on Noncontrast CT Predicts Stroke Subtype and Early Recanalization after Intravenous Recombinant Tissue Plasminogen Activator

BACKGROUND AND PURPOSE: Little is known about the factors that determine recanalization after intravenous thrombolysis. We assessed the value of thrombus Hounsfield unit quantification as a predictive marker of stroke subtype and MCA recanalization after intravenous rtPA treatment.

MATERIALS AND METHODS: NCCT scans and CTA were performed on patients with MCA acute stroke within 4.5 hours of symptom onset. Demographics, stroke severity, vessel hyperattenuation, occlusion site, thrombus length, and time to thrombolysis were recorded. Stroke origin was categorized as LAA, cardioembolic, or indeterminate according to TOAST criteria. Two blinded neuroradiologists calculated the Hounsfield unit values for the thrombus and contralateral MCA segment. We used ROC curves to determine the rHU cutoff point to discriminate patients with successful recanalization from those without. We assessed the accuracy (sensitivity, specificity, and positive and negative predictive values) of rHU in the prediction of recanalization.

RESULTS: Of 87 consecutive patients, 45 received intravenous rtPA and only 15 (33.3%) patients had acute recanalization. rHU values and stroke mechanism were the highest predictive factors of recanalization. The Matthews correlation coefficient was highest for rHU (0.901). The sensitivity, specificity, and positive and negative predictive values for lack of recanalization after intravenous rtPA for $rHU \leq 1.382$ were 100%, 86.67%, 93.75%, and 100%, respectively. LAA thrombi had lower rHU than cardioembolic and indeterminate stroke thrombi ($P = .004$).

CONCLUSIONS: The Hounsfield unit thrombus measurement ratio can predict recanalization with intravenous rtPA and may have clinical utility for endovascular treatment decision making.

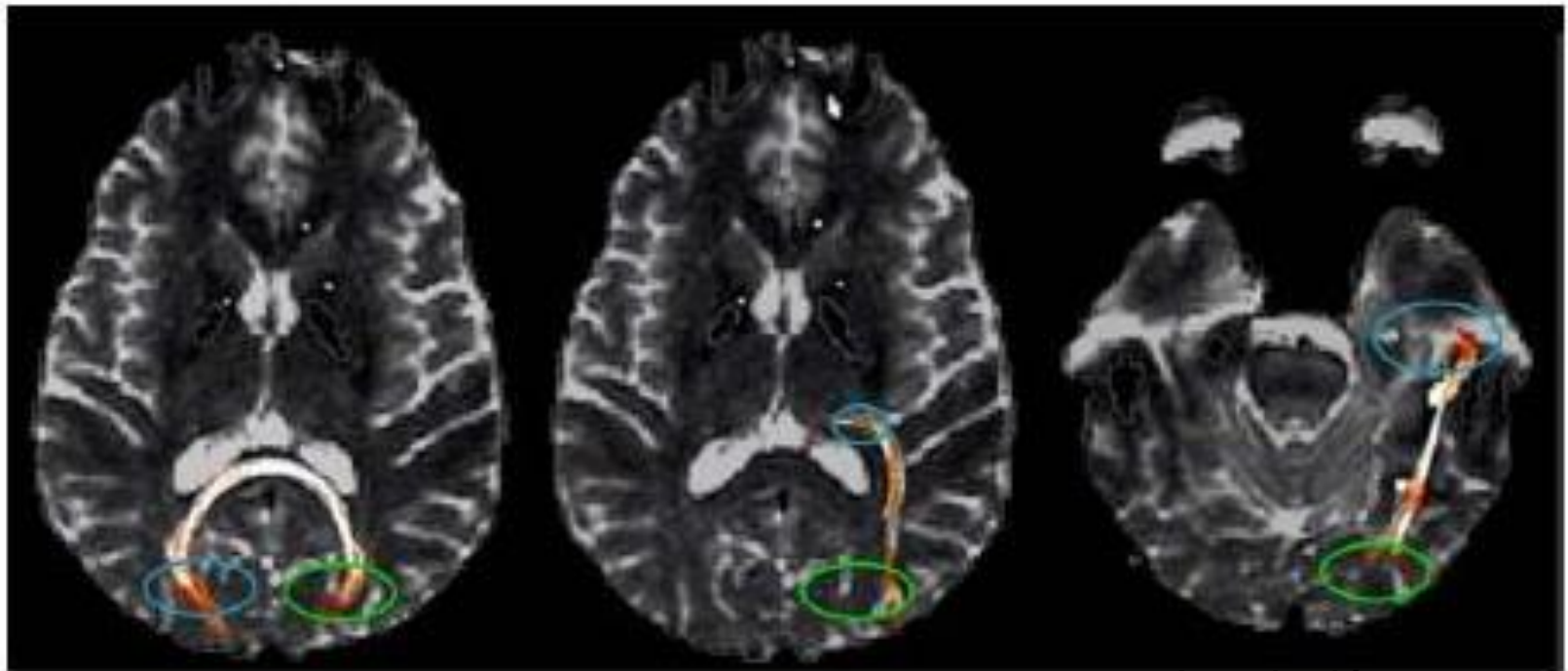
Validació, Qualificació

DTI

¿Anatomía de la Sustancia Blanca?



¿Anatomía de la Sustancia Blanca?



Comisural

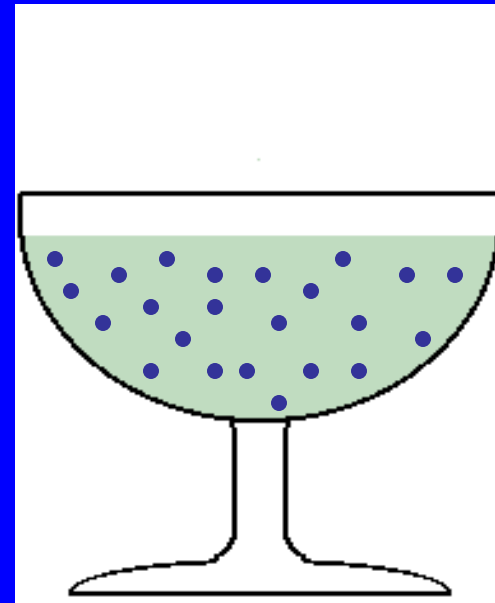
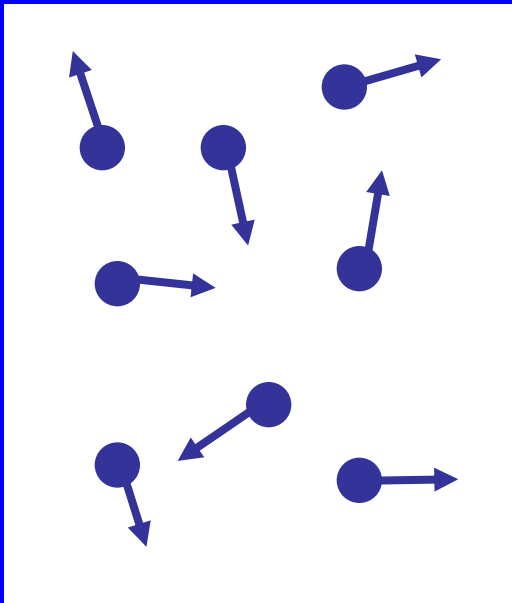
Proyección

Asociación

Mukherjee P et al. Neuroimag Clin N Am 2005; 15:655-665.

Difusió per RM (DRM)

- La Difusió es basa en l'existència d'un moviment aleatori (brownià) de les molècules en estat líquid a través dels compartiments tissulars.



Difusió per RM (DRM)

- **La intensitat de senyal de les imatges de difusió reflecteix el moviment de l'aigua.**

Difusió per RM (DRM)

- La intensitat de senyal de les imatges de

Difusió

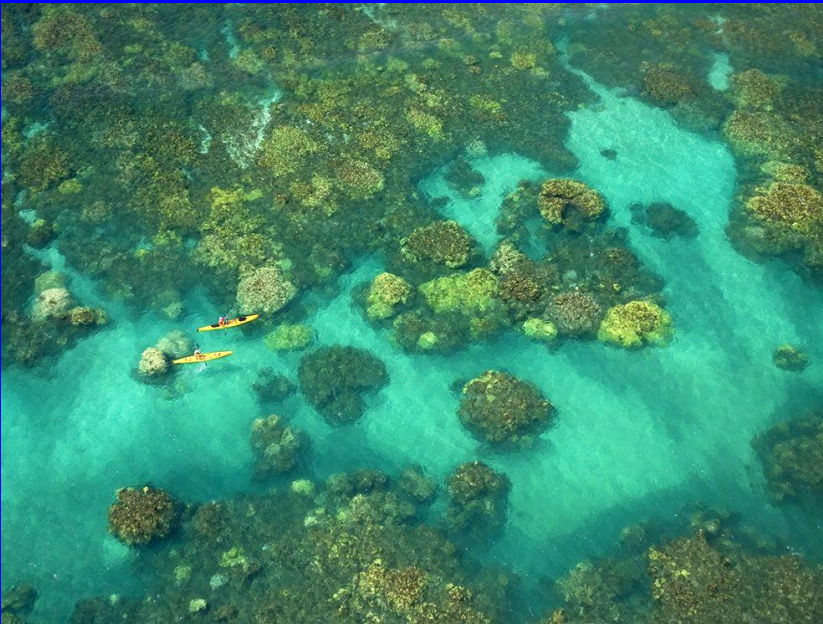
- reflecteix el moviment del

Aigua

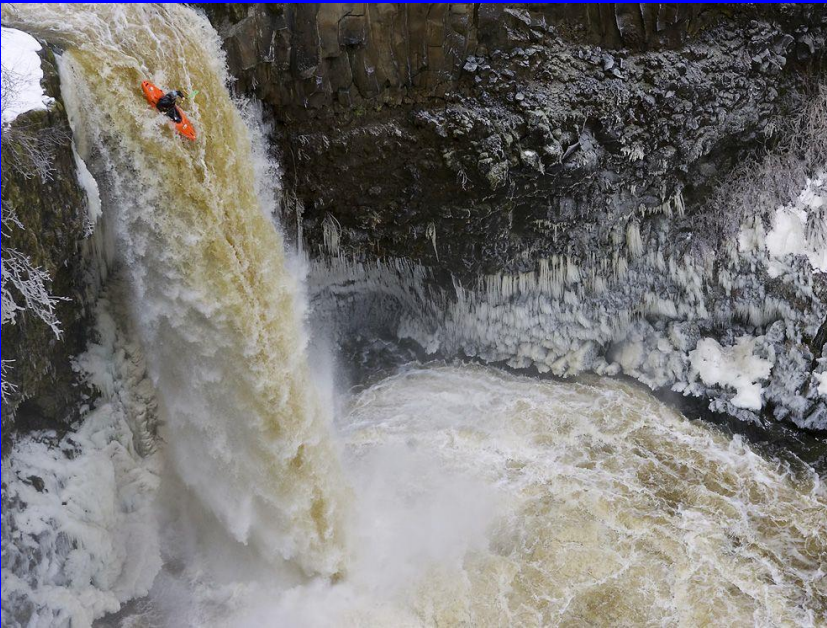
Moviment de l' aigua



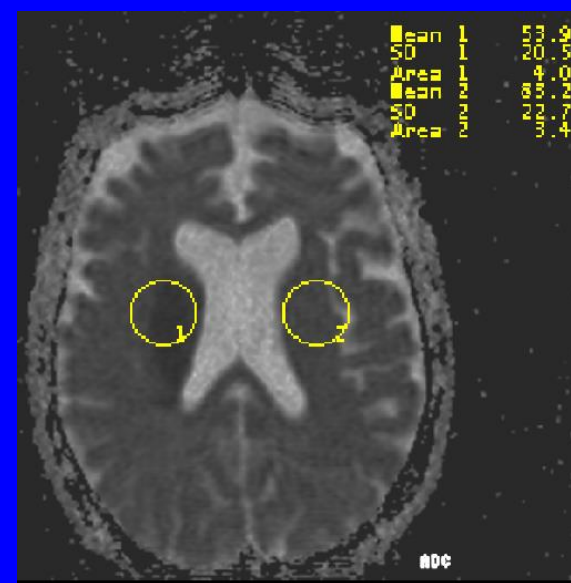
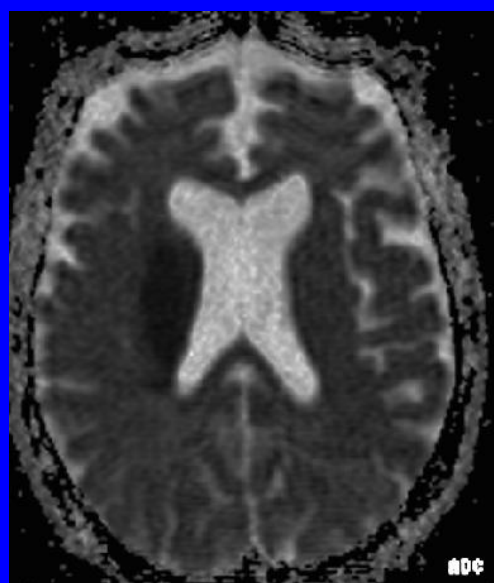
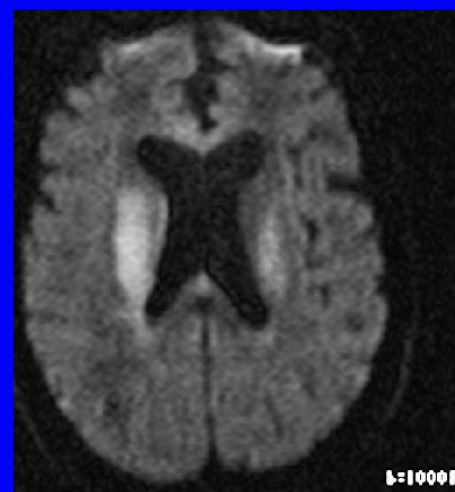
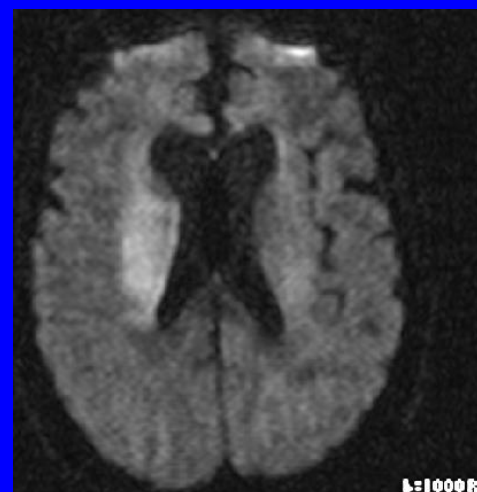
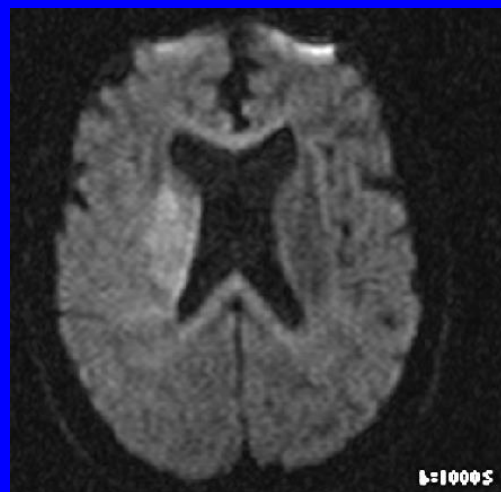
Moviment de l' aigua



Moviment de l' aigua

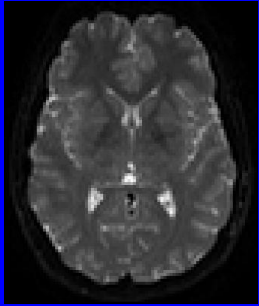


Difusió-trace (DRM)

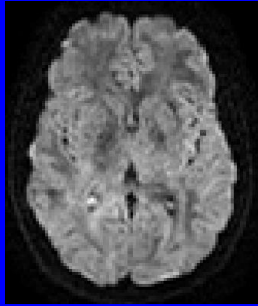


Difusió tensor (mínimo 6 direccions)

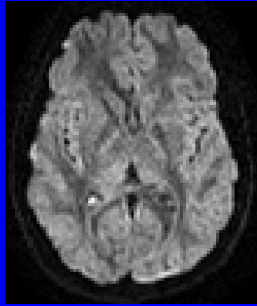
S_0



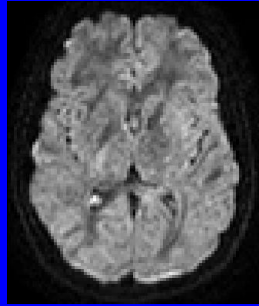
S_1



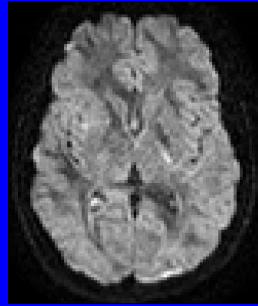
S_2



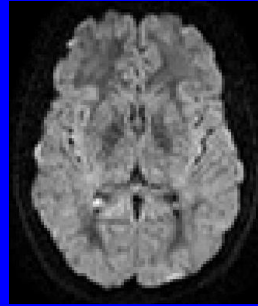
S_3



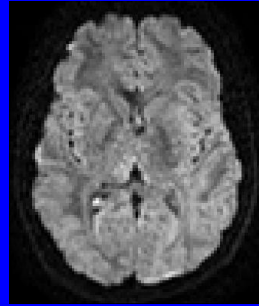
S_4



S_5



S_6



$$g_0 = \begin{pmatrix} 0 \\ 0 \\ 0 \end{pmatrix}$$

$$g_1 = \begin{pmatrix} -1/3 \\ -2/3 \\ -2/3 \end{pmatrix}$$

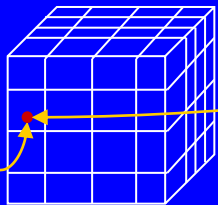
$$g_2 = \begin{pmatrix} -2/3 \\ -1/3 \\ 2/3 \end{pmatrix}$$

$$g_3 = \begin{pmatrix} 2/3 \\ -2/3 \\ 1/3 \end{pmatrix}$$

$$g_4 = \begin{pmatrix} -\sqrt{2}/2 \\ \sqrt{2}/2 \\ 0 \end{pmatrix}$$

$$g_5 = \begin{pmatrix} 0 \\ -\sqrt{2}/2 \\ \sqrt{2}/2 \end{pmatrix}$$

$$g_6 = \begin{pmatrix} \sqrt{2}/2 \\ 0 \\ \sqrt{2}/2 \end{pmatrix}$$

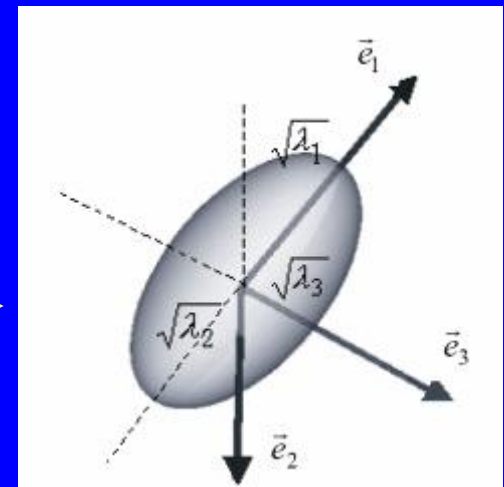


$$\begin{pmatrix} D_{xx} & D_{xy} & D_{xz} \\ D_{yx} & D_{yy} & D_{yz} \\ D_{zx} & D_{zy} & D_{zz} \end{pmatrix}$$

Diagonalització

$$\begin{pmatrix} \lambda_1 & & \\ & \lambda_2 & \\ & & \lambda_3 \end{pmatrix}, \begin{pmatrix} \vec{e}_1 \\ \vec{e}_2 \\ \vec{e}_3 \end{pmatrix}$$

Direcció principal de difusió



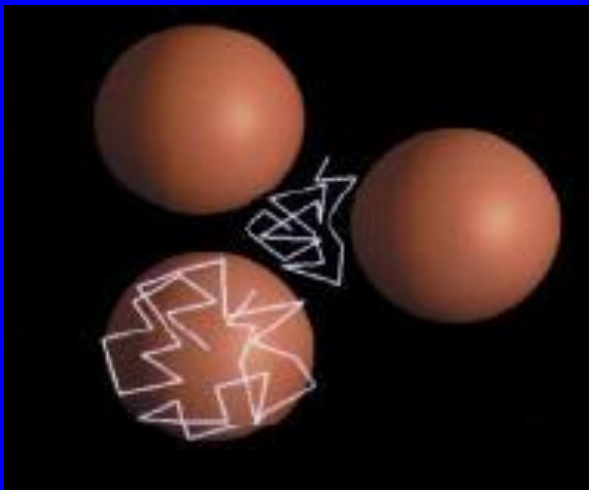
Consecuencias?

- El agua difondeix més lliurement en el pla paral·lel als axons que en el pla perpendicular al mateix.
- Es pot representar com es la difusió i l'anisotropía de cada fibra. :

Difusió-técnica (DRM)

ISOTRÒPICA

- La molècula de Aigua es desplaça en qualsevol direcció.
- Anàlisi de 3 direccions.

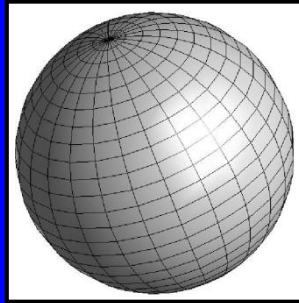
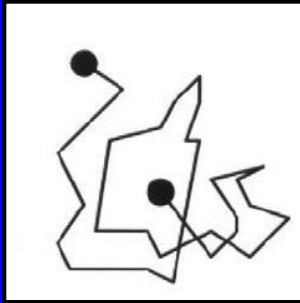


ANISOTRÒPICA

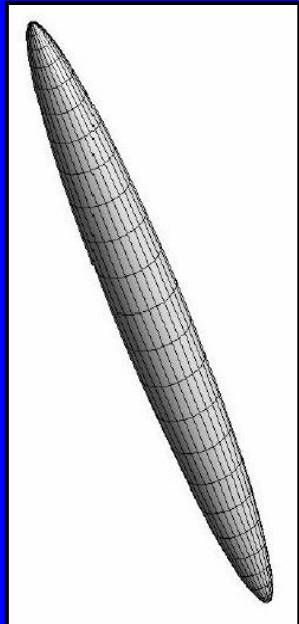
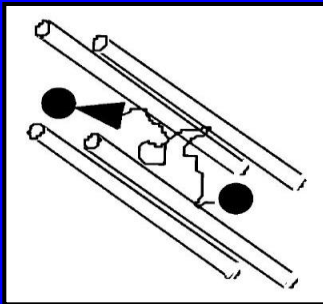
- La molècula d'aigua es desplaça en una direcció predominant.
- Anàlisi de 6,10,16,64 direccions



¿DTI Técnica?

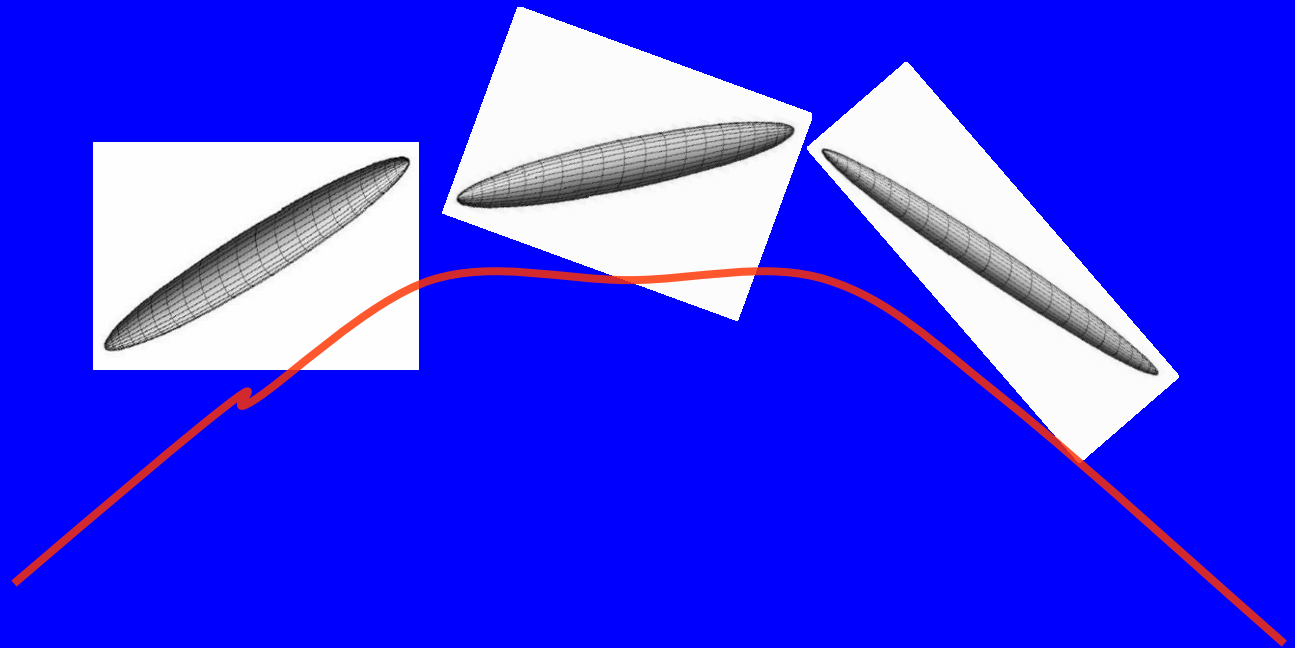
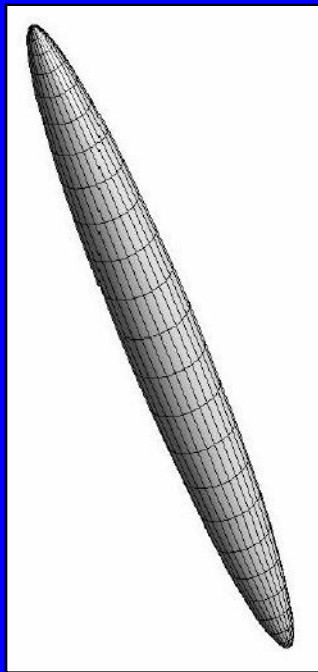


Isotropía



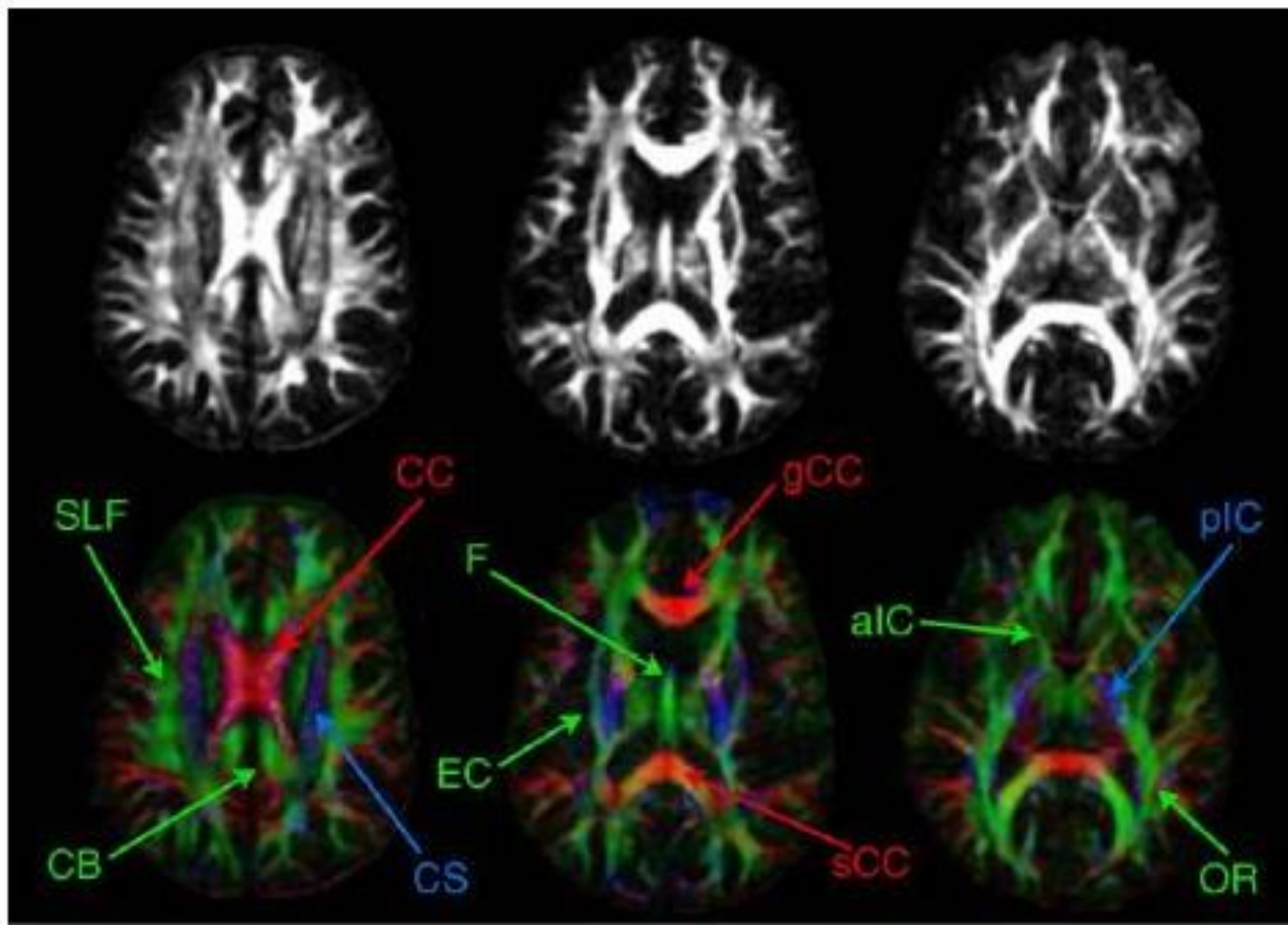
Anisotropía

¿Reconstrucció?



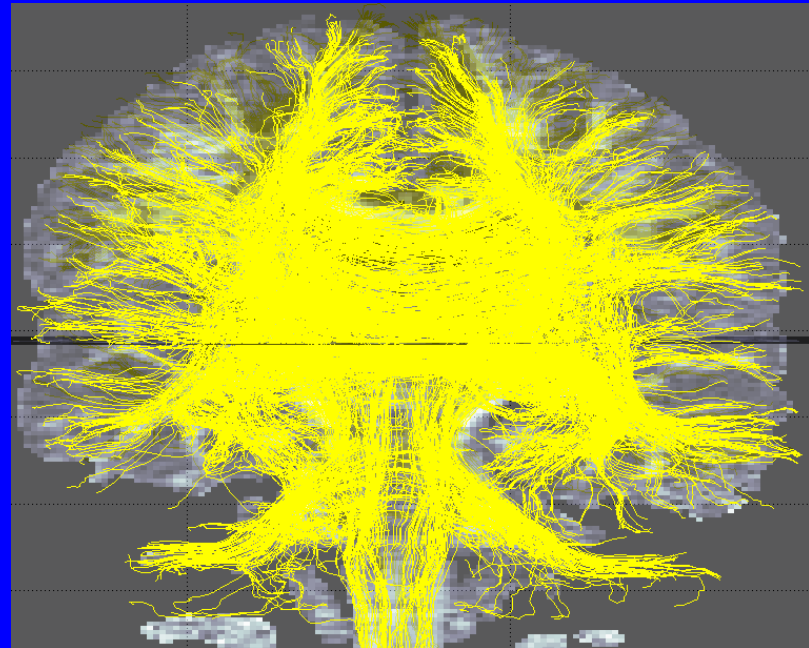
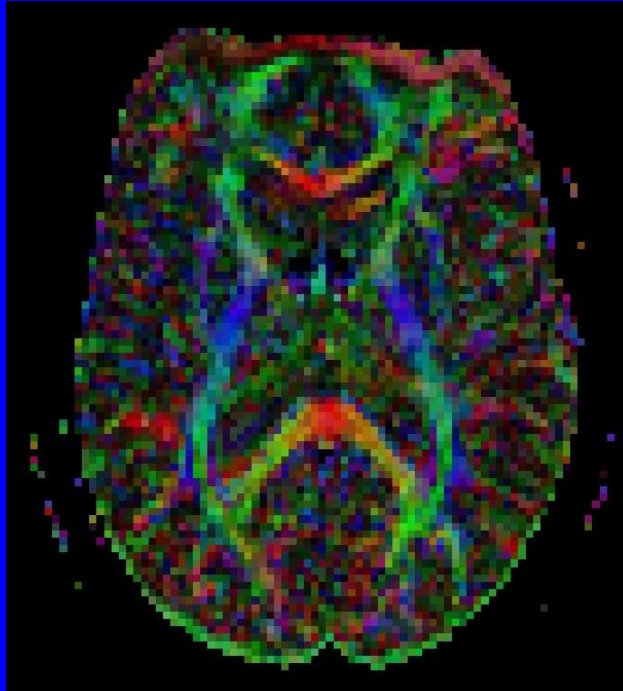
¿Quina informació dona?

- **Sentit de fibres:**
 - Vermell: LR-RL.
 - Verd: AP.
 - Blau: CC.
 - Mezcla en fibras obliques.



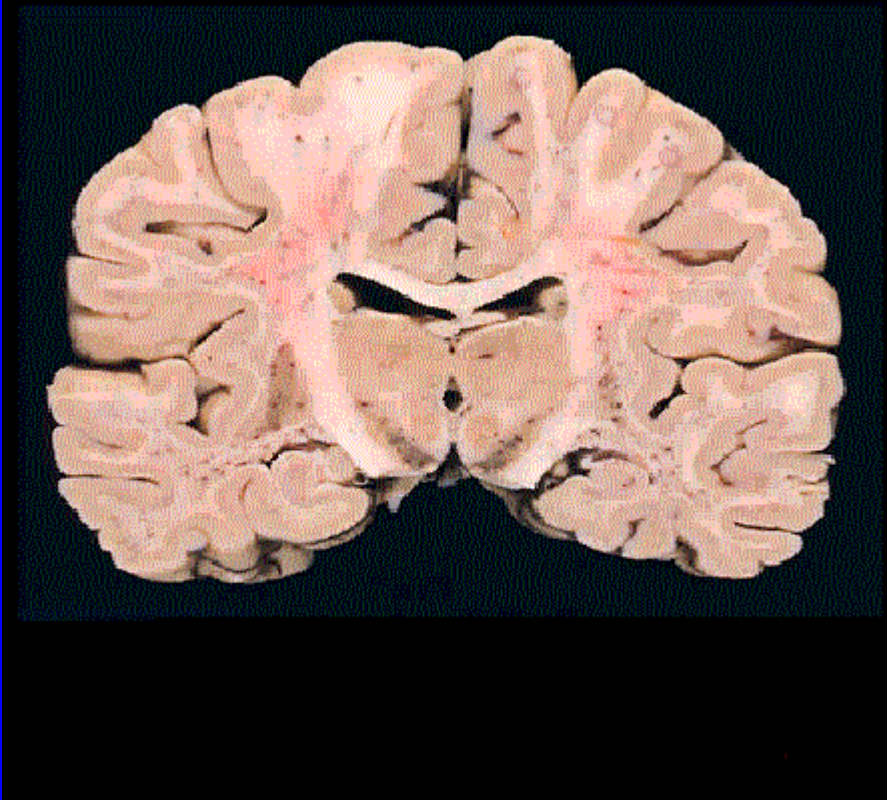
Mukherjee P et al. Neuroimag Clin N AM

Utilitat



- **La DTI mostra la microestructura y organització geomètrica dels teixits.**

DTI

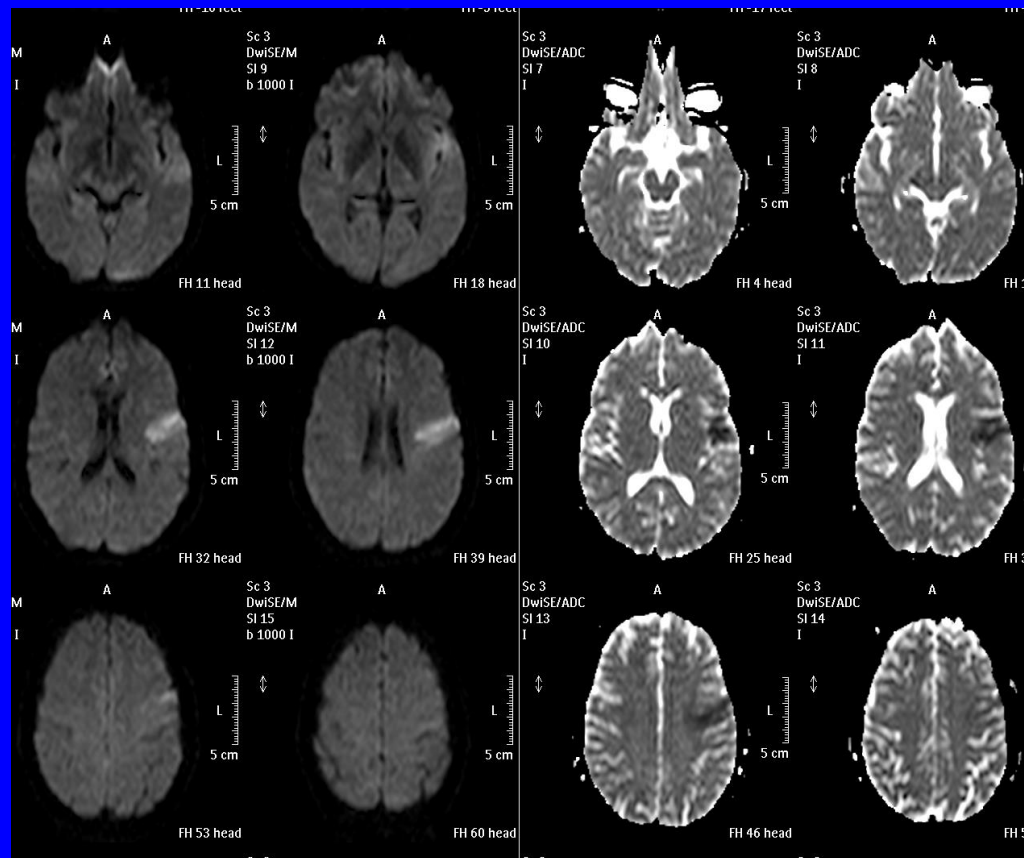


¿Interpretació de DTI?

- Se obtenen 3 tipus de imatges:
 - Difusivity que mesura la difusió global de la difusió independentment de las direcciones.
 - Anisotropía que mesura la diferencia de difusió en diferents direcciones.
 - Tractografía que mesura l' estructura dels tractes de SB.

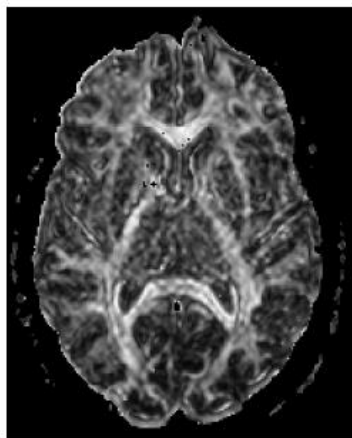
Difusión-técnica (DRM)

ISOTRÒPICA

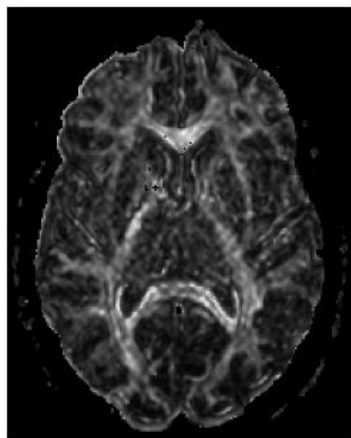


Mapa isotrópico y ADC

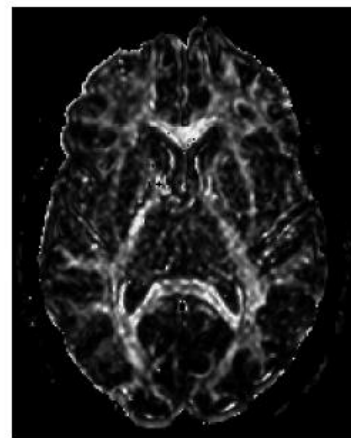
Valors de la DTI



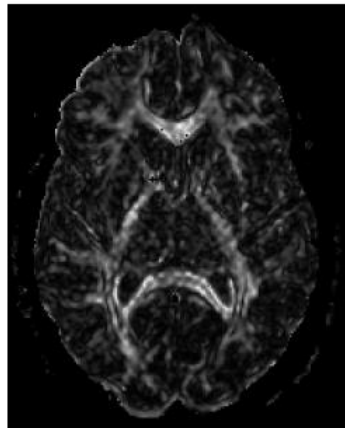
FA



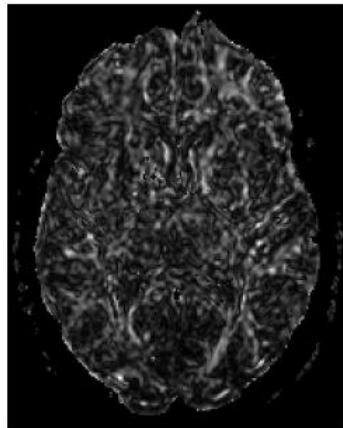
RA



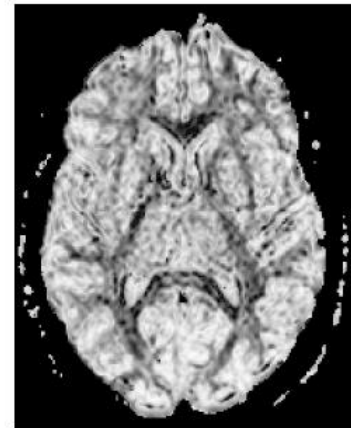
VR



CI



Cp



Cs

Valors de la DTI

Indice	Equation	Meaning
Trace	$trace = \lambda_1 + \lambda_2 + \lambda_3$	The <i>trace</i> can be seen as the orientational diffusivity
Mean diffusivity ($\langle\lambda\rangle$)	$\langle\lambda\rangle = \frac{trace}{3}$	It characterizes the overall mean-squared displacement of molecules and the overall presence of obstacles to diffusion
Fractional Anisotropy (FA)	$FA = \frac{\sqrt{3}}{\sqrt{2}} \frac{\sqrt{(\lambda_1 - \langle\lambda\rangle)^2 + (\lambda_2 - \langle\lambda\rangle)^2 + (\lambda_3 - \langle\lambda\rangle)^2}}{\sqrt{(\lambda_1)^2 + (\lambda_2)^2 + (\lambda_3)^2}}$	FA has been shown to provide the best contrast between different classes of brain tissues
Relative anisotropy (RA)	$RA = \frac{\sqrt{3}}{\sqrt{2}} \frac{\sqrt{(\lambda_1 - \langle\lambda\rangle)^2 + (\lambda_2 - \langle\lambda\rangle)^2 + (\lambda_3 - \langle\lambda\rangle)^2}}{(\lambda_1) + (\lambda_2) + (\lambda_3)}$	Ratio of anisotropy to isotropy
Volume Ratio (VR)	$VR = 1 - \frac{\lambda_1 \lambda_2 \lambda_3}{\langle\lambda\rangle^3}$	Ratio of ellipsoid volume to sphere volume
Cl	$Cl = \frac{(\lambda_1 - \lambda_2)}{\lambda_1 + \lambda_2 + \lambda_3}$	Linear case, anisotropic diffusion. We can observe highly organized white matter regions
Cp	$Cp = \frac{2(\lambda_2 - \lambda_3)}{\lambda_1 + \lambda_2 + \lambda_3}$	Planar case, planar diffusion. It is generally associated with diffusion sheets or may describe regions of crossing fibres
Cs	$Cs = \frac{3\lambda_2}{\lambda_1 + \lambda_2 + \lambda_3}$	Spherical case, isotropic diffusion,. Grey matter and fluids such as CSF

Improved Assessment of *Ex Vivo* Brainstem Neuroanatomy with High-Resolution MRI and DTI at 7 Tesla

GUADALUPE SORIA,^{1,2*} MATTEO DE NOTARIS,^{3,4} RAÚL TUDELA,^{2,5}
GERARD BLASCO,⁶ JOSEP PUIG,⁶ ANNA M. PLANAS,^{1,2}
SALVADOR PEDRAZA,^{6,7} AND ALBERTO PRATS-GALINO³

¹Department of Brain Ischemia and Neurodegeneration, Institut d'Investigacions Biomèdiques de Barcelona (IIBB)-Consejo Superior de Investigaciones Científicas (CSIC), Institut d'Investigacions Biomèdiques August Pi i Sunyer (IDIBAPS), Rosselló 162, Barcelona 08036, Spain

²Experimental MRI 7T Unit, Institut d'Investigacions Biomèdiques August Pi i Sunyer (IDIBAPS), Villarroel 170, Barcelona 08036, Spain

³Laboratory of Surgical Neuroanatomy (LSNA), Facultat de Medicina, Universitat de Barcelona, Casanova 143, Barcelona 08036, Spain

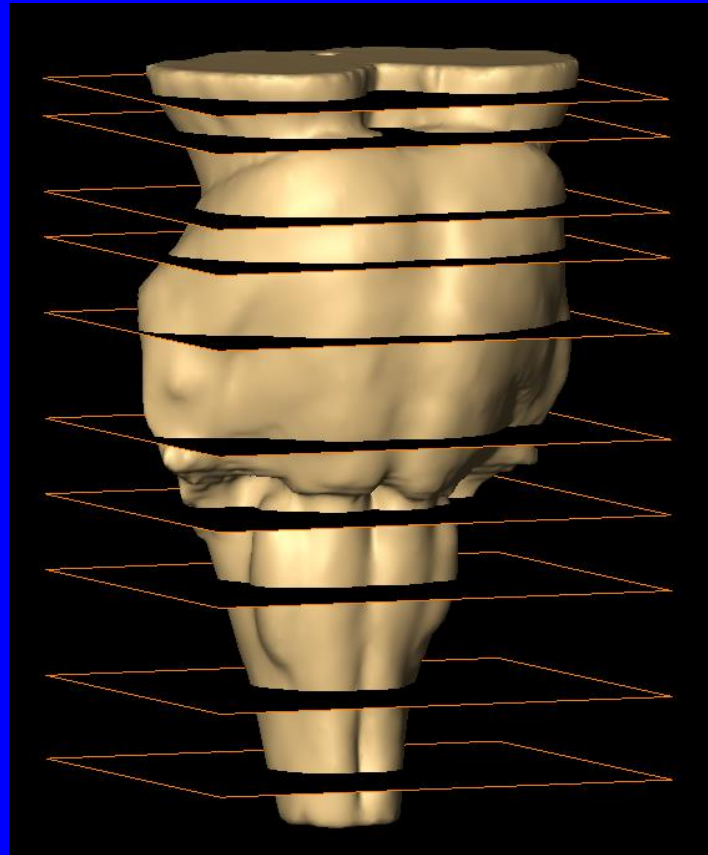
⁴Department of Neurological Sciences, Division of Neurosurgery, Università degli Studi di Napoli Federico II, Via Sergio Pansini 5, Naples 80131, Italy

⁵CIBER de Bioingeniería, Biomateriales y Nanomedicina (CIBER-BBN), Group of Biomedical Imaging of the University of Barcelona, Casanova 143, Barcelona 08036, Spain

⁶IDI, Radiology Department, Hospital Universitario Dr. Josep Trueta. IDIBGI, Universitat de Girona, Av. Francia s/n, Girona 17007, Spain

⁷Programa de Doctorado del Departament de Medicina de la Universitat Autònoma de Barcelona, Passeig Vall d'Hebron, 119, Barcelona 08035, Spain

Topografía de tractos de sustancia blanca y núcleos de sustancia gris en tronco encefálico con RM 7 T.



Superior midbrain (10)

Pontomesencephalic junction (8)

Medium pons (6)

Inferior pons (5)

Superior medulla (4)

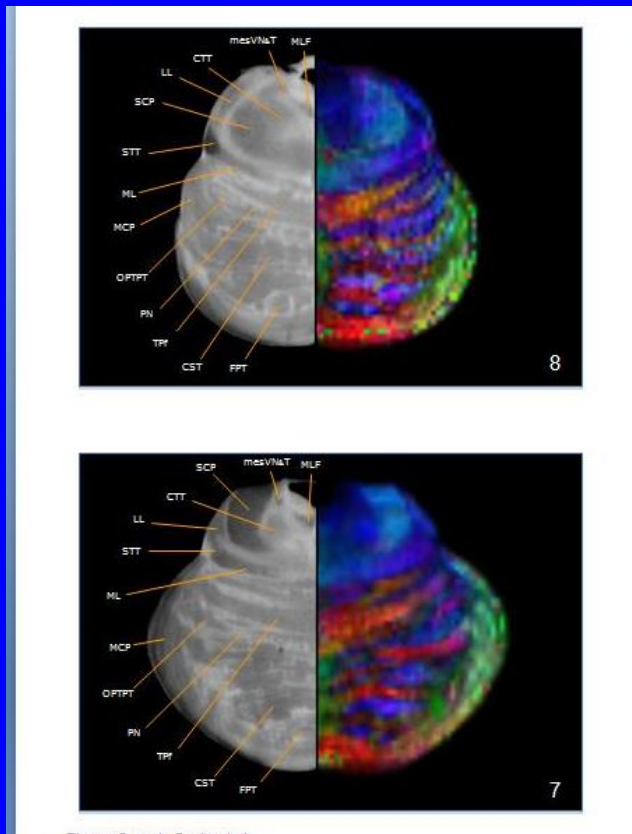
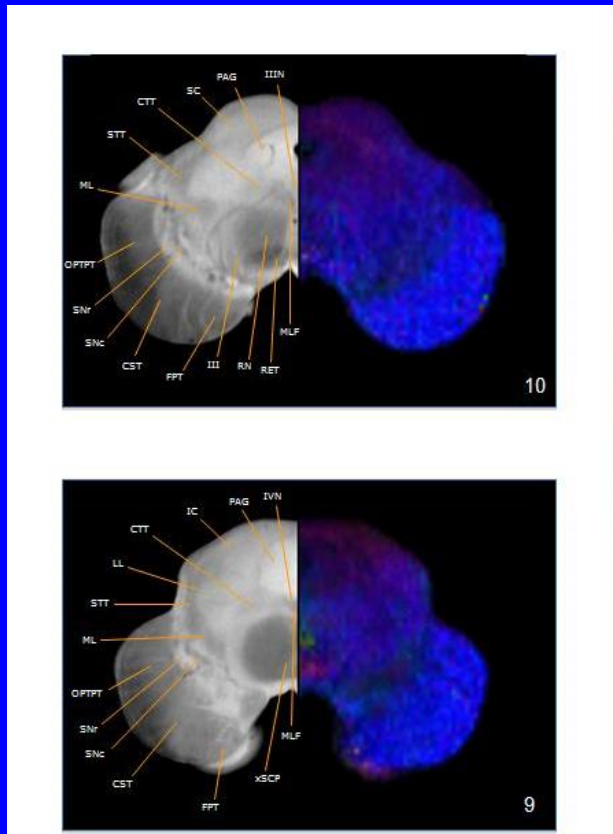
Medium medulla (3)

Inferior medulla (2)

Pyramidal decussation (1)

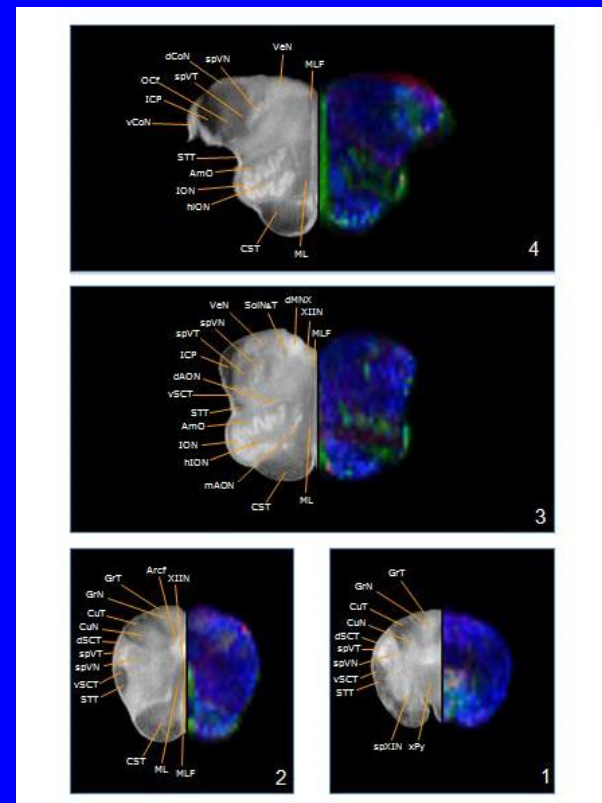
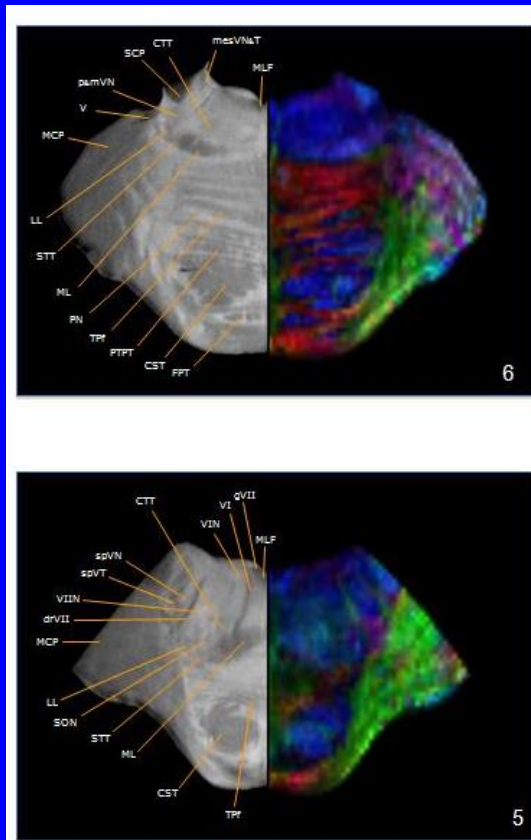
Soria H, de Notaris et al. Improved assessment of ex vivo brainstem neuroanatomy with high resolution MRI and DTI at 7 Tesla. Anatomical record 2011;294:1035-44.

Topògrafia dels tractes de substància blanca amb DTI e imatge estructural

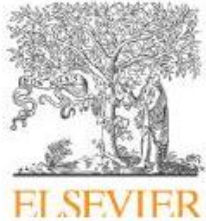


Soria H, de Notaris et al. Improved assessment of ex vivo brainstem neuroanatomy with high resolution MRI and DTI at 7 Tesla. *Anatomical record* 2011;294:1035-44.

La RM de alta resolució determinen amb precisió estructures de tronc que normalment no s'aprecien en equips de baix camp.



Soria H, de Notaris et al. Improved assessment of ex vivo brainstem neuroanatomy with high resolution MRI and DTI at 7 Tesla. Anatomical record 2011;294:1035-44.



Contents lists available at ScienceDirect

Clinical Neurophysiology

journal homepage: www.elsevier.com/locate/clinph



Functional anatomy of subcortical circuits issuing from or integrating at the human brainstem

Alberto Prats-Galino^{a,*}, Guadalupe Soria^{b,c}, Matteo de Notaris^{a,d}, Josep Puig^e, Salvador Pedraza^{e,f}

^a Laboratory of Surgical NeuroAnatomy (LSNA), Facultat de Medicina, Universitat de Barcelona, Barcelona, Spain

^b Experimental MRI 7T Unit, Institut d'Investigacions Biomèdiques August Pi i Sunyer (IDIBAPS), Barcelona, Spain

^c Department of Brain Ischemia and Neurodegeneration, Institut d'Investigacions Biomèdiques de Barcelona (IIBB)-Consejo Superior de Investigaciones Científicas (CSIC), Institut d'Investigacions Biomèdiques August Pi i Sunyer (IDIBAPS), Barcelona, Spain

^d Department of Neurological Sciences, Division of Neurosurgery, Università degli Studi di Napoli Federico II, Naples, Italy

^e IDI, Radiology Department, Hospital Universitario Dr. Josep Trueta, IDIBGI, Universitat de Girona, Girona, Spain

^f Programa de Doctorat. Departament de Medicina. Universitat Autònoma de Barcelona, Spain

Descripció dels circuits de tronc encefàlic amb RM d'alta resolució.

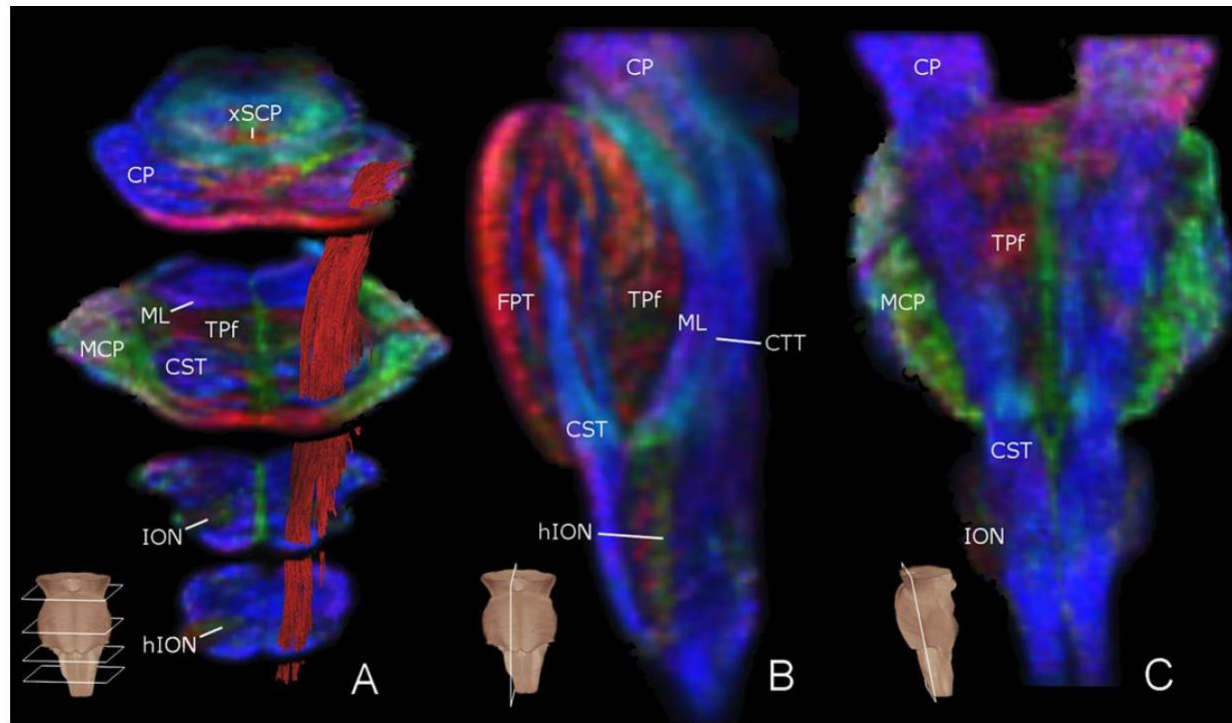


Fig. 7. (A) Tractographic reconstruction of the corticospinal tract along four representative rostrocaudal levels of the brainstem. (B) Coronal section of the brainstem. CP: cerebral peduncle; CST: corticospinal tract; CTT: central tegmental tract; FPT: frontopontine tract; hION: hilum of the ION, containing olivocerebellar fibers; ION: inferior olivary nucleus; MCP: middle cerebellar peduncle; ML: medial lemniscus; TPf: transverse pontine fibers; xSCP: decussation of the superior cerebellar peduncle. RGB maps from DTI of *ex vivo* brainstem at 7 T.

Prats-Galino A et al. Functional anatomy of subcortical circuits issuing from or integrating at the human brainstem. Clinical Neurophysiology 2012;123:4-12.

Descripció dels circuits de tronc encefàlic amb RM d'alta resolució.

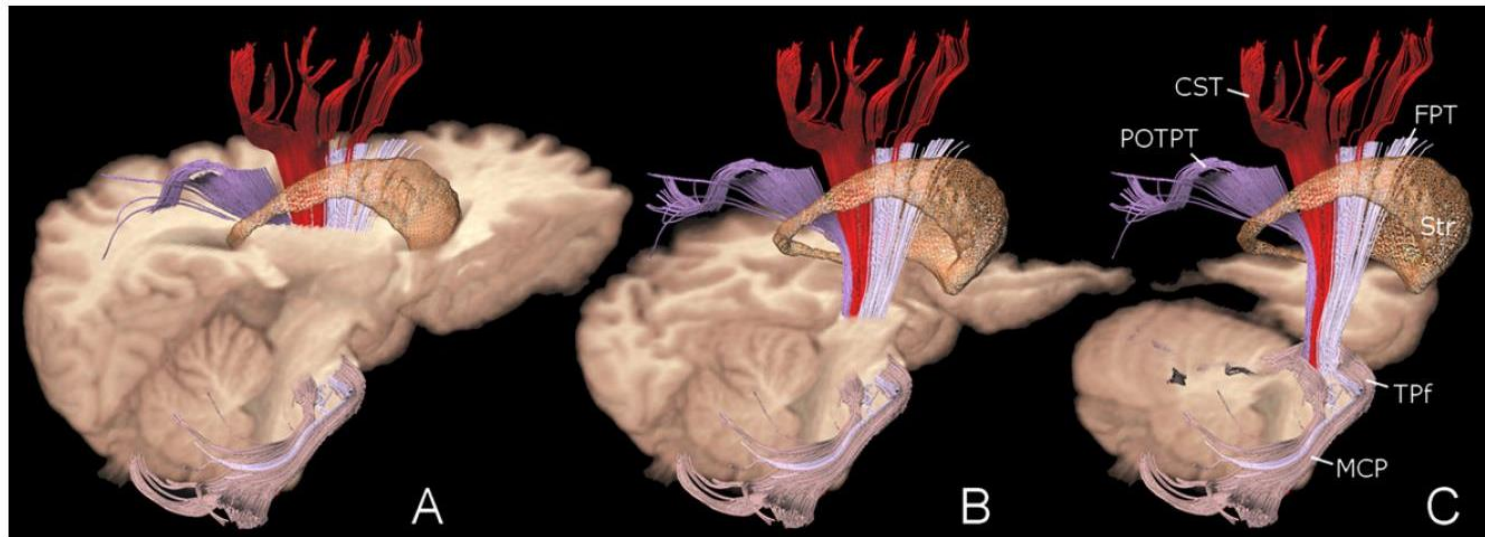


Fig. 8. Tractographic reconstruction of the corticospinal tract, corticopontine tracts and pontocerebellar fiber system within a volumetric rendered model of the left hemisphere properly sectioned to visualize their topographical relationships at: (A) the internal capsule, (B) the cerebral peduncle and (C) the base of the pons levels. Also a mesh surface model of the striatum (Str) is shown. CST: corticospinal tract; FPT: frontopontine tract; MCP: middle cerebellar peduncle; POTPT: parietotemporooccipitopontine; TPf: transverse pontine fibers. Conventional *in vivo* structural MR and DTI study.

Prats-Galino A et al. Functional anatomy of subcortical circuits issuing from or integrating at the human brainstem. Clinical Neurophysiology 2012;123:4-12.

*Information-Theoretic Approach for
Automated White Matter Fiber Tracts
Reconstruction*

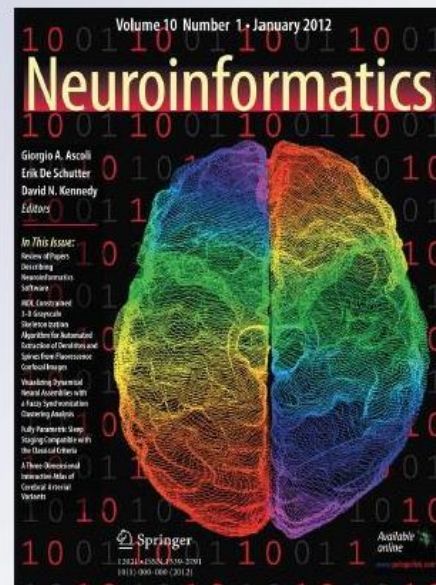
**Ferran Prados, Imma Boada, Miquel
Feixas, Alberto Prats-Galino, Gerard
Blasco, Josep Puig & Salvador Pedraza**

Neuroinformatics

ISSN 1539-2791

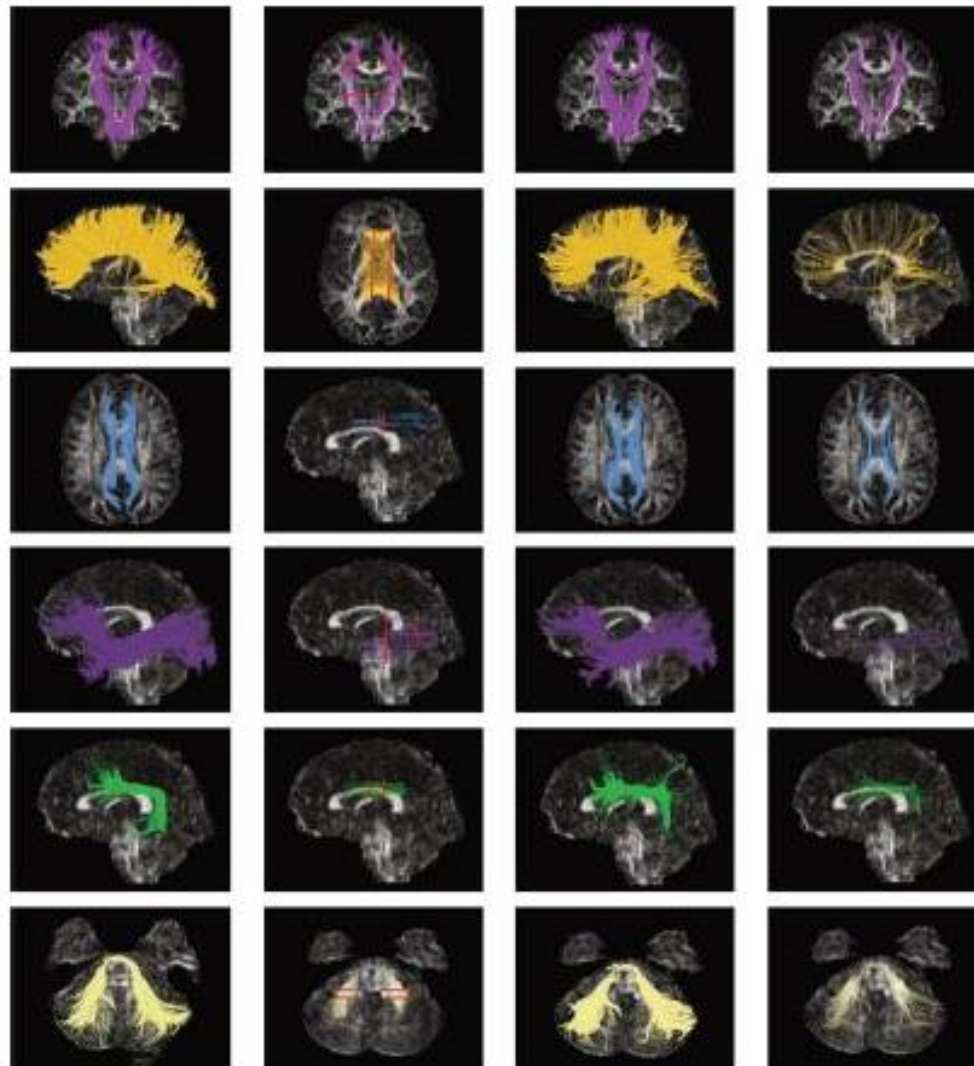
Neuroinform

DOI 10.1007/s12021-012-9148-z



Puig J et al. AJNR 2010 Mar 18. 1324-30

Fig. 8 From *left to right*, we present, for the real DTI data, the manual reconstruction, the VOIs and the reception planes automatically defined with $MIR = 0.4$, and the automated reconstructions with the best and worst agreement, respectively. The evaluated structures are the corticospinal tract, the corpus callosum, the cingulum, the inferior fronto-occipital fasciculus, the superior longitudinal fasciculus, and the middle cerebellar peduncle



Information-Theoretic Approach for Automated White Matter Fiber Tracts Reconstruction

Ferran Prados · Imma Boada · Miquel Feixas ·
Alberto Prats-Galino · Gerard Blasco ·
Josep Puig · Salvador Pedraza

© Springer Science+Business Media, LLC 2012

Abstract Fiber tracking is the most popular technique for creating white matter connectivity maps from diffusion tensor imaging (DTI). This approach requires a seeding process which is challenging because it is not clear how and where the seeds have to be placed. On the other hand, to enhance the interpretation of fiber maps, segmentation and clustering techniques are applied to organize fibers into anatomical structures. In this paper, we propose a new approach to automatically obtain bundles of fibers grouped into anatomical regions. This method applies an information-theoretic split-and-merge algorithm that considers fractional anisotropy and fiber orientation information to automatically segment white matter into volumes of interest (VOIs) of similar FA and eigenvector orientation. For each VOI, a number of planes and seeds is automati-

cally placed in order to create the fiber bundles. The proposed approach avoids the need for the user to define seeding or selection regions. The whole process requires less than a minute and minimal user interaction. The agreement between the automated and manual approaches has been measured for 10 tracts in a DTI brain atlas and found to be almost perfect ($\kappa > 0.8$) and substantial ($\kappa > 0.6$). This method has also been evaluated on real DTI data considering 5 tracts. Agreement was substantial ($\kappa > 0.6$) in most of the cases.

Keywords Diffusion MRI · Tractography · Seeding · White matter

Introduction

Puig J et al. AJNR 2010 Mar 18. 1324-30

**ORIGINAL
RESEARCH**

J. Puig
S. Pedraza
G. Blasco
J. Daunis-i-Estadella
A. Prats
F. Prados
I. Boada
M. Castellanos
J. Sánchez-González
S. Remollo
G. Laguillo
A.M. Quiles
E. Gómez
J. Serena

Wallerian Degeneration in the Corticospinal Tract Evaluated by Diffusion Tensor Imaging Correlates with Motor Deficit 30 Days after Middle Cerebral Artery Ischemic Stroke

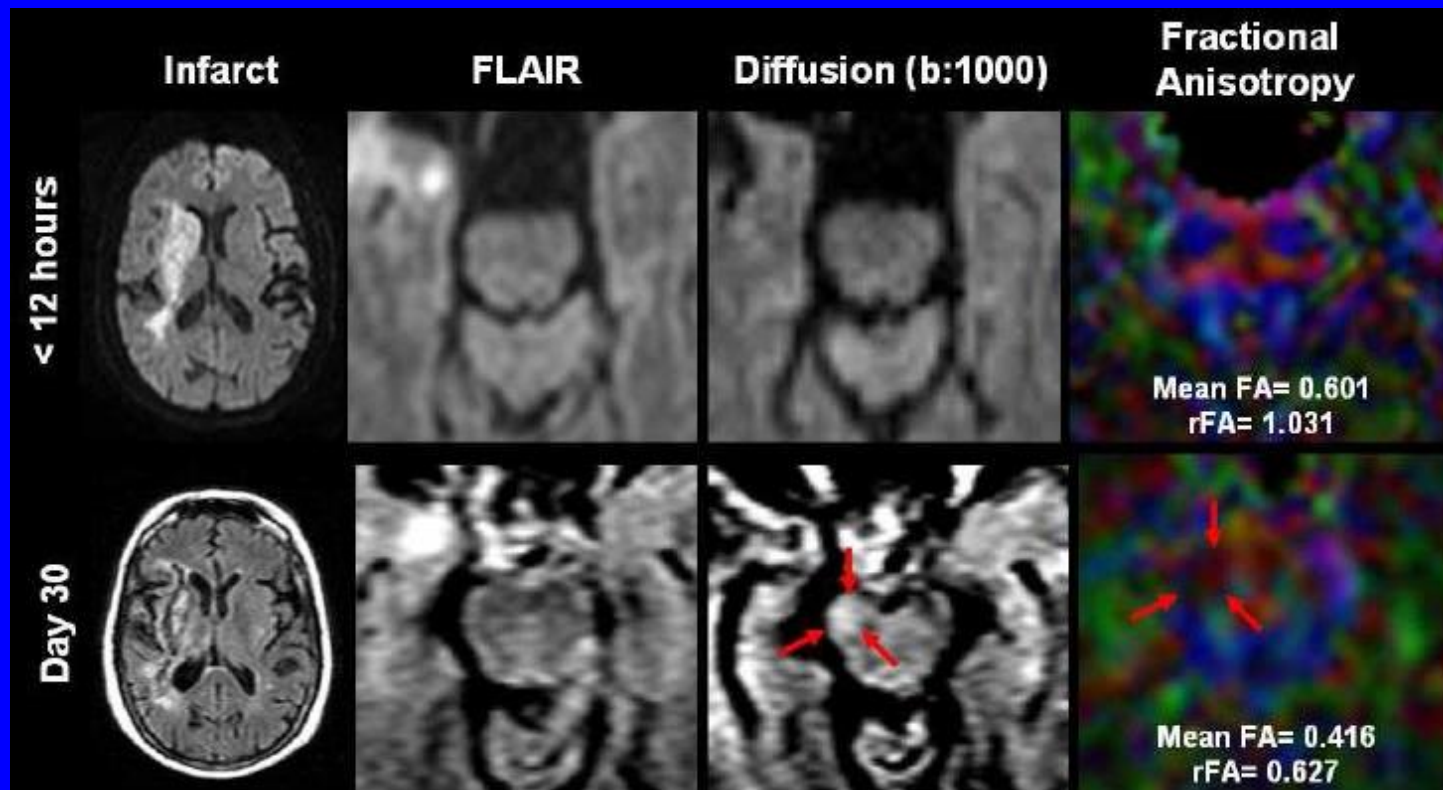
BACKGROUND AND PURPOSE: The quantification and clinical significance of WD in CSTs following supratentorial stroke are not well understood. We evaluated the anisotropy by using DTI and signal-intensity changes on conventional MR imaging in the CST to determine whether these findings are correlated with limb motor deficit in patients with MCA ischemic stroke.

MATERIALS AND METHODS: We studied 60 patients within 12 hours of stroke onset. At admission, day 3, and day 30 of evolution, patients underwent multimodal MR imaging, including DTI sequences. We assessed the severity of limb weakness by using the motor subindex scores (5a, 5b, 6a, 6b) of the m-NIHSS and established 3 groups: I (m-NIHSS scores of 0), II (m-NIHSS, 1–4), and III (m-NIHSS, 5–8). FA values and rFAs were measured on the affected and the unaffected CSTs in the pons.

RESULTS: FA values for the CST were significantly lower on the affected side compared with the unaffected side only at day 30 ($P < .001$), and the rFA was significantly correlated with the motor deficit at day 30 ($P < .001$; $r = -0.793$). The sensitivity, specificity, and positive and negative predictive values for motor deficit by $rFA < 0.925$ were 95.2%, 94.9%, 90.9%, and 97.4%, respectively.

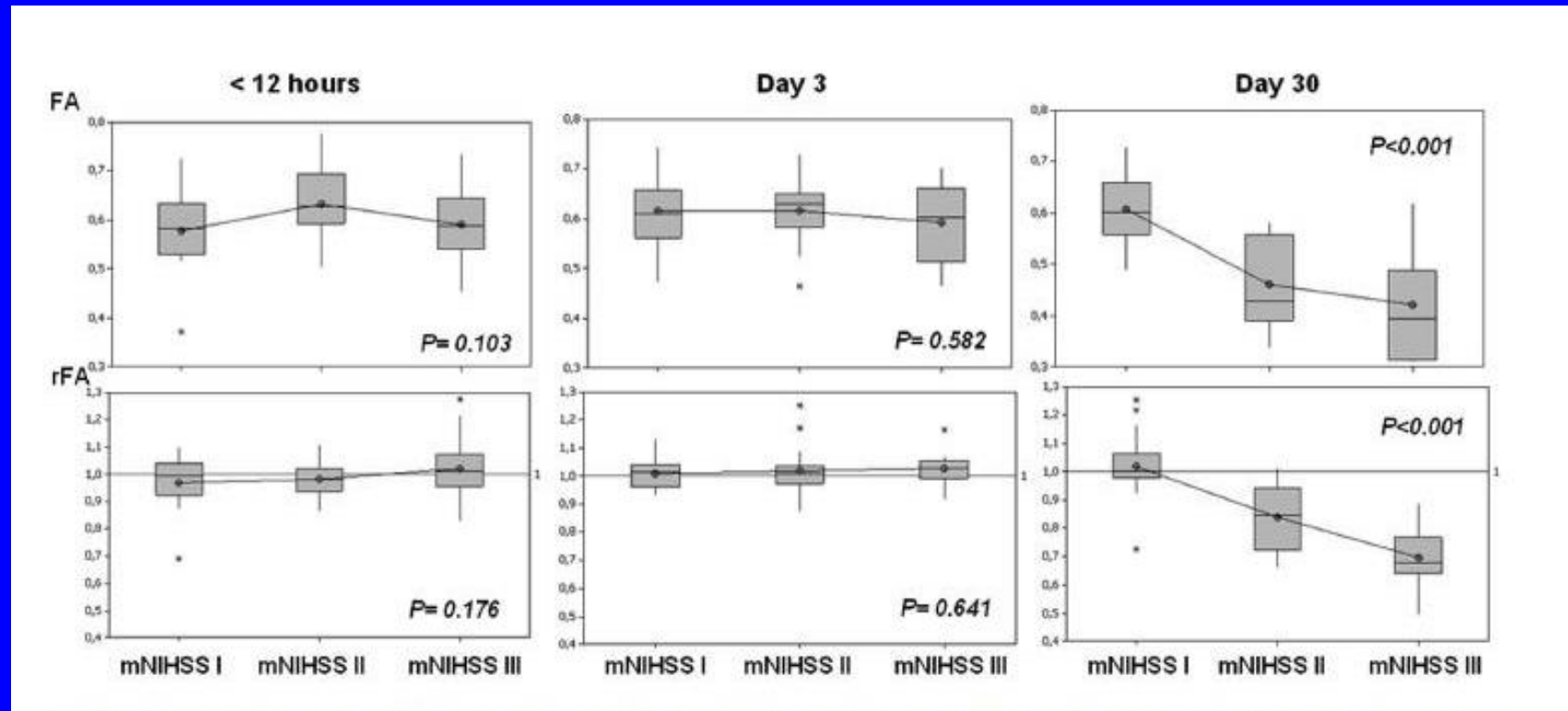
CONCLUSIONS: WD in the CST revealed by DTI correlates with motor deficit 30 days after MCA ischemic stroke. This study highlights the utility of imaging follow-up at 30 days and the potential of DTI as a surrogate marker in clinical trials.

La Degeneració Walleriana de la via piramidal es correlaciona amb una hiperintensitat en difusió (b1000) y una disminució de Anisotropía Fraccional (FA)



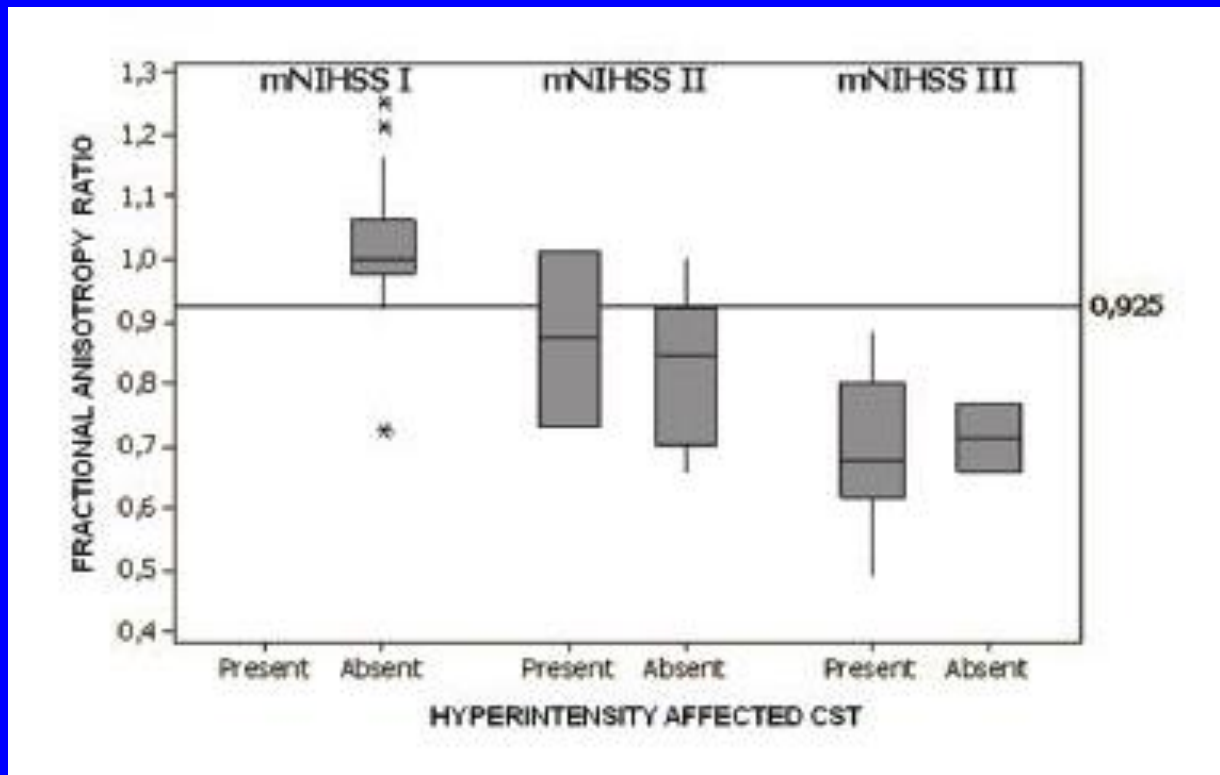
Puig J et al. Wallerian Degeneration in the Corticospinal Tract evaluation by DTI correlates with motor deficit 30 days after MCA ischemic stroke. AJNR 2010.

En el día 30 d'evolució els pacients amb dèficit motor greu mostren una disminució gran de FA i del rati FA.



Puig J et al. Wallerian Degeneration in the Corticospinal Tract evaluation by DTI correlates with motor deficit 30 days after MCA ischemic stroke. AJNR 2010.

La hiperintensitat en FLAIR es poc freqüent. La disminució del FA (rati FA costat patològic/ FA costat sa) es un biomarcador molt més fiable.



Puig J et al. Wallerian Degeneration in the Corticospinal Tract evaluation by DTI correlates with motor deficit 30 days after MCA ischemic stroke. AJNR 2010.

Wallerian Degeneration in the Corticospinal Tract Evaluated by Diffusion Tensor Imaging Correlates with Motor Deficit 30 Days after Middle Cerebral Artery Ischemic Stroke

BACKGROUND AND PURPOSE: The quantification and clinical significance of WD in CSTs following supratentorial stroke are not well understood. We evaluated the anisotropy by using DTI and signal-intensity changes on conventional MR imaging in the CST to determine whether these findings are correlated with limb motor deficit in patients with MCA ischemic stroke.

MATERIALS AND METHODS: We studied 60 patients within 12 hours of stroke onset. At admission, day 3, and day 30 of evolution, patients underwent multimodal MR imaging, including DTI sequences. We assessed the severity of limb weakness by using the motor subindex scores (5a, 5b, 6a, 6b) of the m-NIHSS and established 3 groups: I (m-NIHSS scores of 0), II (m-NIHSS, 1–4), and III (m-NIHSS, 5–8). FA values and rFAs were measured on the affected and the unaffected CSTs in the pons.

RESULTS: FA values for the CST were significantly lower on the affected side compared with the unaffected side only at day 30 ($P < .001$), and the rFA was significantly correlated with the motor deficit at day 30 ($P < .001$; $r = -0.793$). The sensitivity, specificity, and positive and negative predictive values for motor deficit by rFA < 0.925 were 95.2%, 94.9%, 90.9%, and 97.4%, respectively.

CONCLUSIONS: WD in the CST revealed by DTI correlates with motor deficit 30 days after MCA ischemic stroke. This study highlights the utility of imaging follow-up at 30 days and the potential of DTI as a surrogate marker in clinical trials.

**ORIGINAL
RESEARCH**

J. Puig
S. Pedraza
G. Blasco
J. Daunis-i-Estadella
F. Prados
S. Remollo
A. Prats-Galino
G. Soria
I. Boada
M. Castellanos
J. Serena



Acute Damage to the Posterior Limb of the Internal Capsule on Diffusion Tensor Tractography as an Early Imaging Predictor of Motor Outcome after Stroke

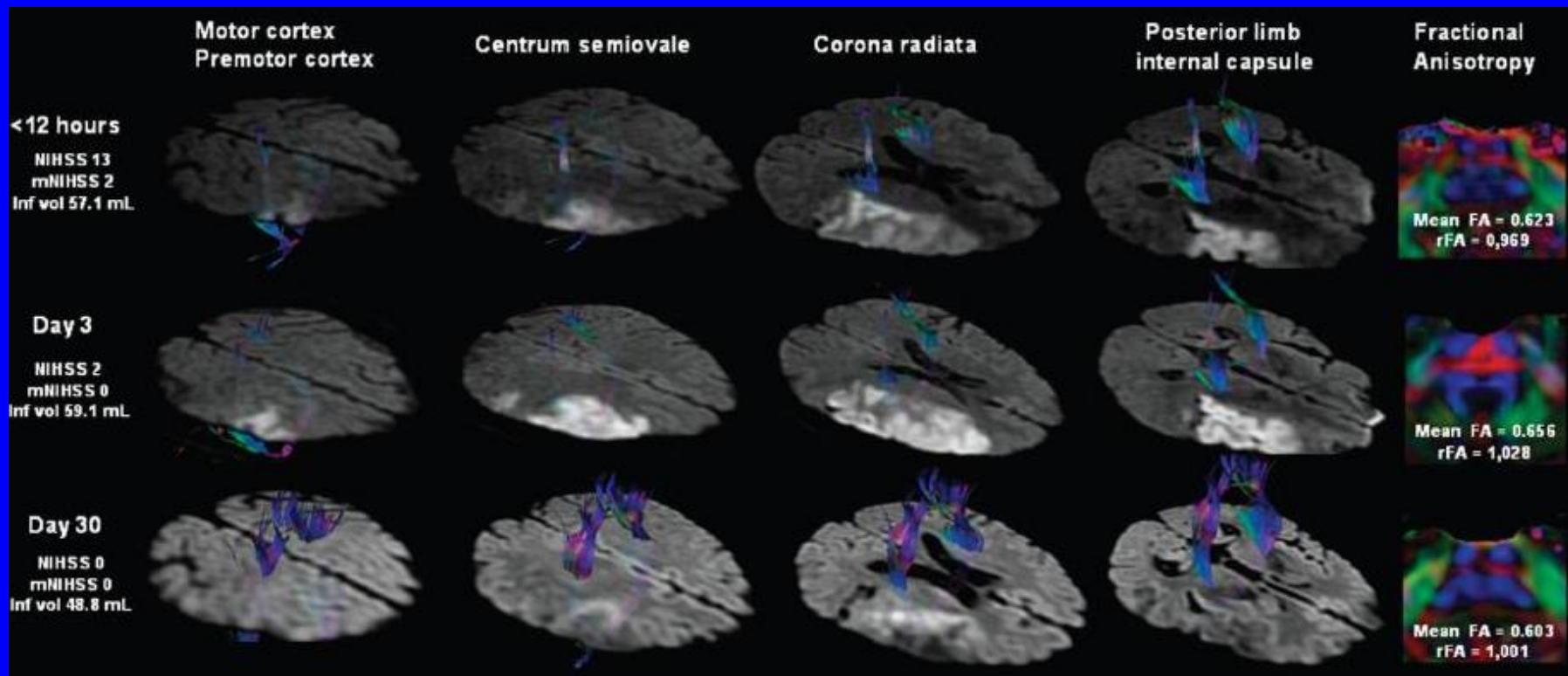
BACKGROUND AND PURPOSE: Early prediction of motor outcome is of interest in stroke management. We aimed to determine whether lesion location at DTT is predictive of motor outcome after acute stroke and whether this information improves the predictive accuracy of the clinical scores.

MATERIALS AND METHODS: We evaluated 60 consecutive patients within 12 hours of middle cerebral artery stroke onset. We used DTT to evaluate CST involvement in the motor cortex and premotor cortex, centrum semiovale, corona radiata, and PLIC and in combinations of these regions at admission, at day 3, and at day 30. Severity of limb weakness was assessed by using the motor subindex scores of the National Institutes of Health Stroke Scale (5a, 5b, 6a, 6b). We calculated volumes of infarct and fractional anisotropy values in the CST of the pons.

RESULTS: Acute damage to the PLIC was the best predictor associated with poor motor outcome, axonal damage, and clinical severity at admission ($P < .001$). There was no significant correlation between acute infarct volume and motor outcome at day 90 ($P = .176$, $r = 0.485$). The sensitivity, specificity, and positive and negative predictive values of acute CST involvement at the level of the PLIC for motor outcome at day 90 were 73.7%, 100%, 100%, and 89.1%, respectively. In the acute stage, DTT predicted motor outcome at day 90 better than the clinical scores ($R^2 = 75.50$, $F = 80.09$, $P < .001$).

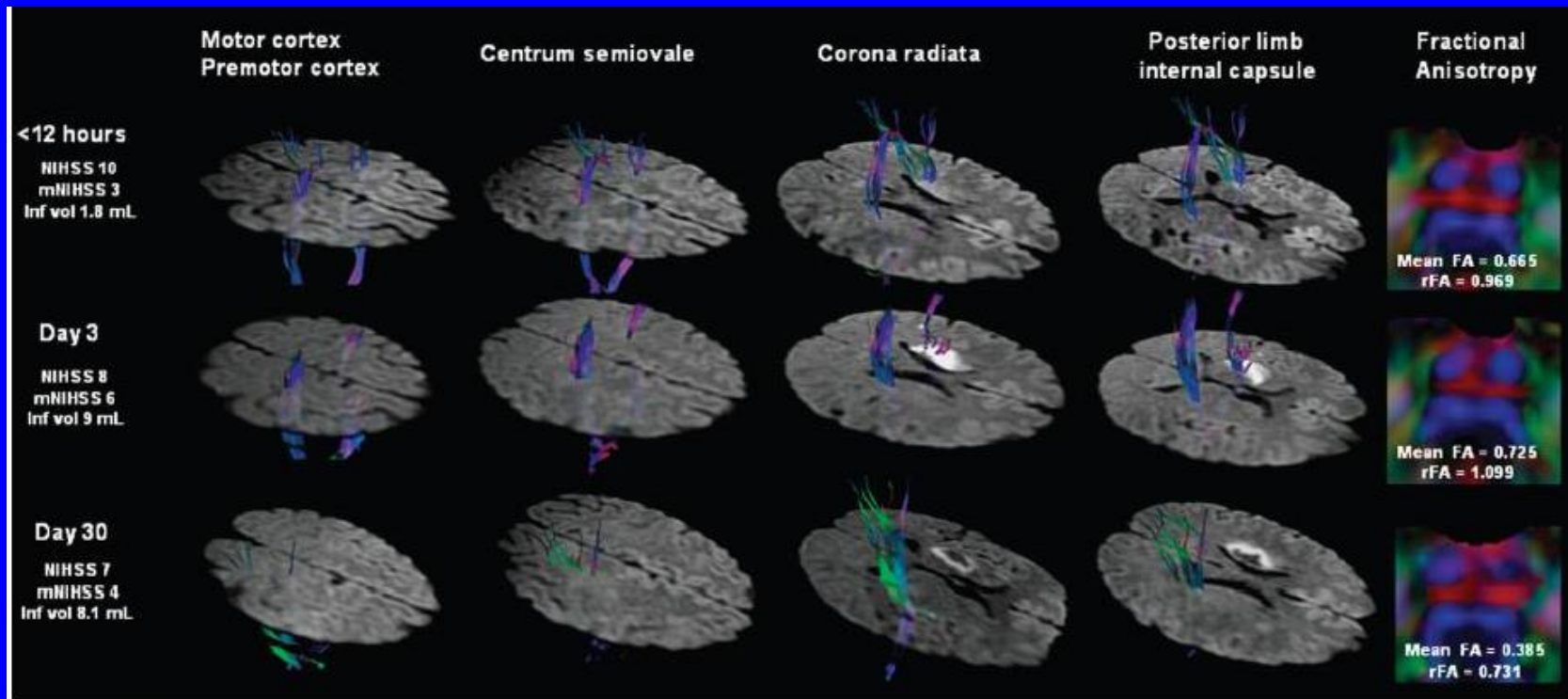
CONCLUSIONS: In the acute setting, DTT is promising for stroke mapping to predict motor outcome. Acute CST damage at the level of the PLIC is a significant predictor of unfavorable motor outcome.

Un gran infart que no afecti al braç posterior de capsula interna No produeix degeneració walleriana i dona poc dèficit motor.



Puig J et al. Acute damage to the Posterior Limb of the Internal Capsule on DTT as an early imaging predictor of motor outcome after stroke. AJNR 2011.

Un petit infart que SI afecti al braç posterior de capsula interna SI produeix degeneració walleriana i dona important dèficit motor.



Puig J et al. Acute damage to the Posterior Limb of the Internal Capsule on DTT as an early imaging predictor of motor outcome after stroke. AJNR 2011.

Acute Damage to the Posterior Limb of the Internal Capsule on Diffusion Tensor Tractography as an Early Imaging Predictor of Motor Outcome after Stroke

BACKGROUND AND PURPOSE: Early prediction of motor outcome is of interest in stroke management. We aimed to determine whether lesion location at DTT is predictive of motor outcome after acute stroke and whether this information improves the predictive accuracy of the clinical scores.

MATERIALS AND METHODS: We evaluated 60 consecutive patients within 12 hours of middle cerebral artery stroke onset. We used DTT to evaluate CST involvement in the motor cortex and premotor cortex, centrum semiovale, corona radiata, and PLIC and in combinations of these regions at admission, at day 3, and at day 30. Severity of limb weakness was assessed by using the motor subindex scores of the National Institutes of Health Stroke Scale (5a, 5b, 6a, 6b). We calculated volumes of infarct and fractional anisotropy values in the CST of the pons.

RESULTS: Acute damage to the PLIC was the best predictor associated with poor motor outcome, axonal damage, and clinical severity at admission ($P < .001$). There was no significant correlation between acute infarct volume and motor outcome at day 90 ($P = .176$, $r = 0.485$). The sensitivity, specificity, and positive and negative predictive values of acute CST involvement at the level of the PLIC for motor outcome at day 90 were 73.7%, 100%, 100%, and 89.1%, respectively. In the acute stage, DTT predicted motor outcome at day 90 better than the clinical scores ($R^2 = 75.50$, $F = 80.09$, $P < .001$).

CONCLUSIONS: In the acute setting, DTT is promising for stroke mapping to predict motor outcome. Acute CST damage at the level of the PLIC is a significant predictor of unfavorable motor outcome.

Utilitat de la DTI en l'infart cerebral.

Premi de la ESNR.

Josep Puig Alcántara

Puig J et al. Wallerian Degeneration in the Corticospinal Tract evaluation by DTI correlates with motor deficit 30 days after MCA ischemic stroke. AJNR 2010.

Puig J et al. Acute damage to the Posterior Limb of the Internal Capsule on DTT as an early imaging predictor of motor outcome after stroke. AJNR 2011.



Proyectos de Investigación.

Ensayos Clínicos.

Artículos.

Tesis doctorales

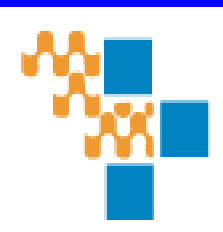
Organización de cursos

Conferencias/Clases

Comunicaciones.

Premios

Centro de referencia internacional.





INFART CEREBRAL

12 Projectes de recerca.

1 FIS: Predicció per RM del Ictus cerebral progressiu.

2 FIS: Utilitat DTI en el maneig de malalt amb infart.

1 FIS: Validació de l' estudi de la permeabilitat.

1 Projecte Europeu (VI programa marc). Iknow.

Desenvolupament de programa d' ajuda al maneig de l'ictus.

1 Projecte Europeu (VII programa marc). Wake-up. Utilitat de RM per tractaments de ictus del despertar.



Difusió pública mitjans de comunicació

O.J.D.: 183067
E.G.M.: 63000
Tarifa: 35.997 €

LA VANGUARDIA
GIRONA

Fecha: 17/02/2012
Sección: ECONOMIA
Páginas: 1-3

DIAGNOSI VITAL NOVES LÍNIES D'INVESTIGACIÓ MÈDICA AL JOSEP TRUETA DE GIRONA

LA PATOLOGIA
Cada any arriben al Trueta de mitjana 70 pacients amb infarts cerebrals

INVESTIGACIÓ
La recerca permet accelerar el trasllat dels pacients que no reaccionaran

de saber d'on trada quan però, o no, es fa un primer tractament en els pacients que arriben a urgències amb un infart cerebral. El doctor del IDI, que després a la vegada de l'IDIBGI (Institut d'Investigació Biomèdica de Girona), ha aconseguit disminuir a través de la radiologia quin tipus de tumors són efectius a l'rtFA i, de la mateixa manera, determinar on pot veure l'infart. És a dir, si s'ha originat des dels arrels carotídes (zona del coll) o del cor. "Com més ràpida és la resposta i més ràpidament es recupera el flux

UNITAT D'IMATGE
L'infermer i tècnic en resonància magnètica, Gerard Blasco, amb un pacient a punt de fer un TAC. En primer terme, una de les imatges obtingudes del cervell del pacient

RENOVANT LA RADIOLOGIA

anquirí al teixit cerebral menys, discapacitats i seqüeles i quedaran al pacient", apunta Puig.

L'origen d'aquesta investigació va començar en una jornada de guiada del doctor Josep Puig al servei d'urgències de l'Hospital Josep Trueta. Explica que un dia hi van arribar, en poc temps, dos pacients amb símptomes evidents que patien un infart cerebral. "Van arribar amb dos trossos visualment molt similars però un es va despertar amb l'rtFA i l'altre no". "Què està passant?", es va preguntar. Al·lucinat va pujar al servei de radiologia i va comprovar que els "trossos" que travesaven l'un i de l'altre eren diferents". És a dir, que tenien una composició diferent. "Poden venir més o menys grans o petits vermells, per exemple", apunta. I, per tant, "l'infart de l'rtFA també seria diferent", afegit.

A partir d'aquí, el responsable d'aquesta investigació va es-

UNA CARRERA JOVE
Ànima de recerca

Josep Puig és un investigador jove que fins i tot, en certs moments de la seva carrera professional, ha hagut de tirar per camins que no li garantien una seguretat ni econòmica ni laboral amb l'objectiu de poder dedicar-se al que de veritat l'apassiona: la recerca. "Això requereix temps, però el temps és limitat i sempre l'acabes pagant amb el teu temps l'ure i el temps en família", reconeix. D'aquesta manera, li ha sortit més que bé ja que amb només cinc anys com a investigador ha publicat fins a tres recerques que han estat reconegudes internacionalment i per aquest

sol·licita en té algunes a punt de sortir del forn.

El bé dit, però, han arribat gràcies a la seva tenacitat i després de rebre un contracte fixo a un cop finalitzada la residència. "Vaig rebre un pas d'assistència per aportar per la recerca", Puig, que és l'única investigadora de l'IDIBGI de l'Hospital Josep Trueta, reconeix que per ell la recerca és com una "droga". "Un cop finalitzada, no la pots deixar", afirma. Lamenta, però, el poc suport que reb en el part de l'administració pública. Actualment, les seves investigacions estan obertes gràcies a fons de recerca europeus.

L'EQUIP. El doctor de l'Institut de Diagnòstic per la Imatge de l'IDIBGI, Josep Puig, analitza una imatge amb l'infermer i tècnic en resonància magnètica, Gerard Blasco

CONCLUSIO

**Hem validat i qualificat
biomarcadors d'imatge i això pot
millorar el diagnòstic, pronòstic
i tractament de pacients amb
infart cerebral**

Thanks



Girona (SPAIN)

